Advances in Bioresorbable Electronics and Uses in Biomedical Sensing

Michelle Kuzma, Ethan Gerhard, Dingying Shan, and Jian Yang

1 Introduction to Bioresorbable Electronics

1.1 Motivation and Classification

More than 46 million tons of electronic waste (e-waste) are produced every year worldwide [67]. E-waste produced by the USA alone exceeds five million tons with similar amounts produced by other developing and established markets [67, 103]. Given the fast turnover of technology and increasing use of electronics in daily life, the rate of e-waste growth was startlingly three times higher than that of any other waste stream in 2016 with only 15–20% being recycled [4, 15, 67, 119]. Healthcare-related electronics furthermore contribute to the growing e-waste epidemic. Unprecedented advanced systems, such as infusion pumps, enhanced bioimaging, wireless communication, dialysis machines, electronic healthcare records, and long-term, implantable electronic devices, such as the cardioverter defibrillator, ventricular assist devices, and brain-instrument interfaces, became emerging essentials to patient care over the course of the twentieth century [15, 37, 106]. Despite the vast strides made in clinical care due to these rising technologies, soft, *biodegradable* electronic implants remained a clear, unmet need, with only flexible non-electronic biodegradable implants or non-resorbable electronic implants that not only added to e-waste accumulation, but contributed to adverse patient outcomes including tissue obstruction due to rigid designs, limited sensitivity from poor device tissue contact, and foreign body responses in addition to iatrogenic

M. Kuzma
Department of Materials Science and Engineering, Materials Research Institute, The Pennsylvania State University, University Park, PA, USA

E. Gerhard · D. Shan · J. Yang (✉)
Department of Biomedical Engineering, Materials Research Institute, The Huck Institutes of The Life Sciences, The Pennsylvania State University, University Park, PA, USA
e-mail: jxy30@psu.edu

H. Cao et al. (eds.), *Interfacing Bioelectronics and Biomedical Sensing*,
https://doi.org/10.1007/978-3-030-34467-2_2

complications from surgical removal, like infection, tissue damage, psychological distress, and superfluous costs widely available [15, 59].

It was not until Hwang and colleagues reported a state-of-the-art proof-of-concept electronic device composed of thin layers of silk with magnesium (Mg), magnesium oxide (MgO), silicon dioxide (SiO_2), and monocrystalline silicon nanomembranes (Si-NMs) that the first entirely transient electronic device was realized (Fig. 1) [36]. The device demonstrated successful engineering of both soluble *active components* (i.e., transistors) and [49] *passive components* (i.e., resistors, inductors, capacitors). The fabricated device was capable of energy storage, wireless heating, and imaging, demonstrating that this technology could have versatile and unprecedented utility in many biomedical applications [36, 49]. The bioresorbable materials were used in concert to comprise active and passive components with corresponding interconnects placed onto a silk substrate that visibly degraded in as little as 5 minutes into nontoxic and non-immunogenic by-products [35, 36]. Furthermore, this study established the critical finding that the device and degradation by-products were safe in vivo, sparking inspiration to revolutionize implantable electronics for acute, clinical scenarios while reducing healthcare-related e-waste [36].

Following this breakthrough, the class of *transient electronics* came to fruition. Although transient electronic systems often incorporate materials used in conventional, nondegradable electronics, the components in transient devices are nanometers to micrometers in dimension, which enables complete degradation within

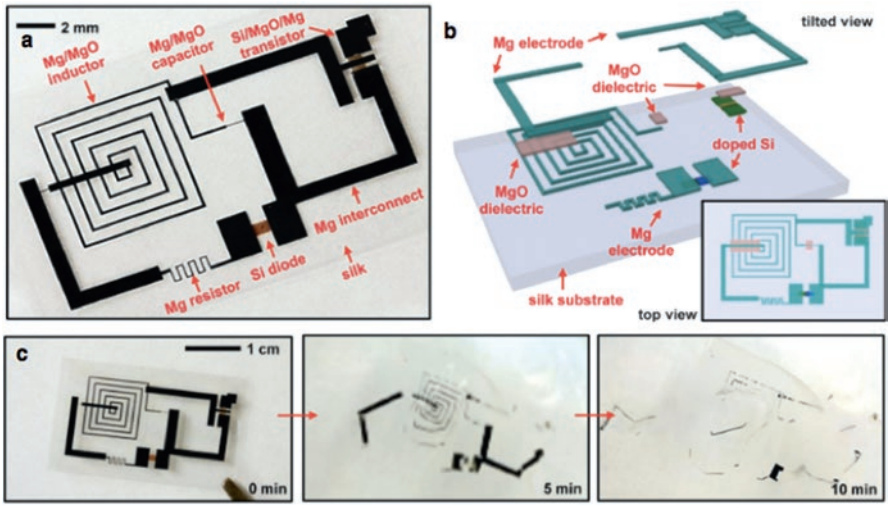

Fig. 1 (**a**) The first fully bioresorbable electronic system with engineered active and passive components using thin films of magnesium (Mg), magnesium oxide (MgO), and silicon (Si) on a silk substrate (**b**) Exploded schematic of the resorbable device and an inset containing a top view. (c) Demonstrated transience of the device upon immersion in DI water within 10 minutes. (From Hwang et al. [36]. Reprinted with permission from AAAS)

minutes to days under benign conditions [59]. The bulk materials used in traditional silicon-based electronics, on the contrary, hydrolyze at negligible rates on the order of nanometer's per day [59]. Therefore, distinct from traditional built-to-last electronics, transient electronics encompass electronic devices capable of disappearing by degradation or dissolution in a controllable manner over relevant timeframes in benign environmental conditions [6, 78, 116].

The terms transient electronics and biodegradable electronics are used to describe degradable or resorbable devices with applications in and beyond the biomedical field (i.e., environmental sensing, solar cells, self-degrading data security systems, and photodetectors) [59, 78]. Meanwhile, *bioresorbable electronics* frequently refers to the subdivision of transient electronics that safely disappear in the body [59, 62, 119]. Likewise, in this chapter, the same classification of bioresorbable electronics will be adopted to describe the biomedical cohort of transient and biodegradable electronic systems.

1.2 Background

Prior to the advent of the first completely biodegradable electronic device, increased attention was devoted to small-scale material deposition techniques and flexible organic electronics [23, 48, 102] and the development of organic light-emitting devices (OLEDs), thin-film transistors (TFTs), and thin film organic photovoltaic cells, among other flexible microdevices at the end of the Twentieth century [23, 48, 102]. Furthermore, successes in transfer printing in 2006 enabled electronic devices with components that are sensitive to traditional, harsh integrative circuit (IC) fabrication conditions (i.e., vacuum or high temperature) possible [86, 119]. These milestones in flexible electronic production were imperative to the creation of electronic implants that conform to curvilinear shapes of body tissues without resulting in mechanical injury to the surrounding tissue or the device [62]. Meanwhile, water-soluble electronics were being developed during this time. Reported partially soluble devices included organic thin-film transistors (OTFTs), biodegradable organic field-effect transistors (OFETs), stretchable complementary metal-oxide-semiconductor (CMOS) circuits on plastic substrates, and elastic monocrystalline silicon (mono-Si) electronic mesh designs [5, 48, 61].

Furthermore, nonelectronic, resorbable technology (i.e., surgical sutures, cardiovascular stents, tissue scaffolds, drug delivery vehicles, and orthopedic equipment) were emerging at the turn of the twentieth century [15, 119]. However, biodegradable implants possessing electronic capabilities were limited by the absence of active resorbable components capable of sensing, processing, communication, and actuation [15, 37]. The first implantable electronic device with partial bioresorption was reported circa 2010, a single crystal (monocrystalline, single crystalline) silicon-based n-channel metal oxide semiconductor (nMOS) transistor, which incorporated insoluble electrical components on a fully resorbable silk substrate [62]. Although this device functioned successfully in an aqueous environment, was

non-immunogenic, and only possessed finite amounts of insoluble materials, it still necessitated a secondary surgery to remove the insoluble components [62]. It was the collective findings of Si-NMs and metal thin films soluble in water in appreciable timeframes and flexible Si electronics that led to the first fully bioresorbable Si electronic device using CMOS technology in 2012.

Successive innovations in production of transient, soft electronics established utility biomedical engineering applications including photothermal therapy, on-demand drug release, multifunctional vascular stents, intracranial pressure monitoring, temperature monitoring, electrical stimulation, and biosensing [14, 39, 66, 97, 119]. Despite the many advances since the first bioresorbable device, research is ongoing to achieve multifunctional bioresorbable electronics, refine on-demand transience, and develop economical and scalable manufacturing processes for commercialization as well as to study long-term physiological and environmental effects of by-products [14, 15, 34, 72, 119].

The main types of materials used in bioresorbable electronics include thin layers of biodegradable polymers, dielectrics, semiconductors, and conductors [119]. Depending on the material properties, each material can serve different roles or multiple roles from a physical foundation to a protective layer for electronic components or contribute to charge transfer. Many of the properties, such as dissolution rate, electrical performance, and biocompatibility of materials used in transient electronics, have been studied under various conditions [59, 119]. The basic components and properties of respective materials that have developed into current, mainstream transient electronics will be outlined in detail (Sect. 2).

To date, mechanisms of transience in biodegradable electronics include dissolution, degradation, hydrolysis, corrosion, and enzymatic breakdown in response to stimuli including heat, water moisture, aqueous solutions, acid, enzymes, and light [14, 62, 105, 119]. The main types of degradation mechanisms for complete dissolution of implantable bioresorbable electronics are hydrolysis and dissolution in aqueous media [27]. Rate of transiency can be regulated through materials selection and processing, device design, and environmental conditions [119].

2 Overview and Advancements of Constituent Resorbable Materials

Evaluation of the fundamental bioresorbable materials and ensuing innovations moving transient electronics toward practical advanced degradable medical devices are explored in this section in terms of device components (i.e., conductor, semiconductor, dielectric, substrate, and encapsulating layers). Core materials comprising each component are inorganic and/or organic in nature exhibiting conducting, semiconducting, dielectric, and/or insulating properties (Fig. 2) [14, 27, 35, 78, 119]. Material choice for each component is governed by the desired properties (i.e., mechanical, thermal, magnetic, optical, electric, or chemical) needed to generate

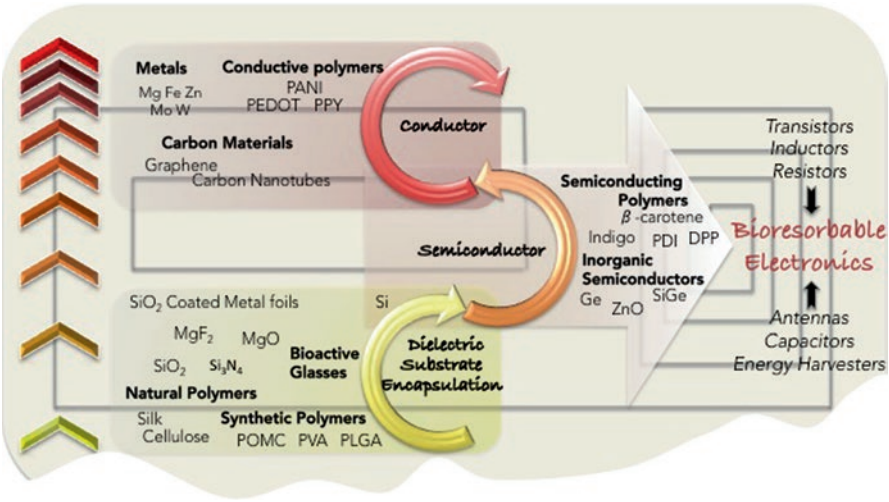

Fig. 2 Key materials used to create functioning components that constitute bioresorbable electronic devices. Materials are divided into three main categories: insulators (i.e., dielectric, substrate, and encapsulating materials), semiconductors, and conductors, with increasing levels of conductivity directed from the bottom to the top of the figure. Silicon (Si) is represented between the semiconductor and insulator windows due to its successful employment as a semiconductor and an encapsulating layer, respectively. (Adapted with permission from Hwang et al. [42]. Copyright 2015 American Chemical Society)

necessary cooperative performance for translatable applications [10]. Further modification through functionalization, engineering, and processing inspired by the established principles reviewed here guides progress in this field for medical advances (Sect. 3) [14].

A property vital to any functioning electronic device is *electrical conductivity*, a second rank tensor that relates the current density to the electric field intensity according to Ohm's law (Eq. 1) [10, 107]:

$$J = \sigma\xi, \tag{1}$$

where J is the current density, σ is the electrical conductivy, and ξ is the electric field intensity [10]. Electrical conductivity is the degree to which electrically charged particles move (i.e. electron, hole, ion, or charged vacancy) within a material in response to an applied electric field [10, 107]. Movement of charged particles, in turn, provokes and dictates the magnitude of an electric current through the material [10, 107]. How easily electrons are available for conduction with respect to energy can be visualized through energy band diagrams [10, 107]. Simply put, conducting materials typically have overlapping valence and conduction bands so that electrons are readily available for conduction, whereas in solid semiconducting and insulating materials, there is a distinct energy barrier electrons must overcome to become involved in conduction (i.e., the energy band gap) [10, 107]. Semiconducting mate-

rials generally have a bandgap of less than two electron volts (eV), while insulators, on the other hand, possess band gaps normally greater than 2 eV [10, 107]. Consequently, conducting materials exhibit the highest conductivities of 10^4–10^7 Siemens per minute (S/m), semiconductors have conductivities ranging from 10^{-6} to 10^4 S/m, while insulators have the lowest conductivities of 10^{-10}–10^{-20} S/m [10]. Dielectric materials are a subset of insulating materials that spontaneously displace charge, or exhibit polarization, in the presence of an electric field [10, 107].

It is as imperative to consider biocompatibility as well as mechanical and chemical properties as it is to evaluate electrical properties in bioresorbable devices to satisfy application requirements (Table 1). Constituent material, the collective device, and degradation by-products must be nontoxic and elicit minimal immune response all while mimicking the flexibility, softness, and/or responsiveness of target tissues and dissolving in a predetermined timeframe [62, 119].

2.1 Conductor

Both conductive inorganic and organic materials have been used in transient electronics as functional materials for interconnects and electrodes [27, 119]. The inorganic and organic materials used as conducting components in bioresorbable electronics accompanied by pertinent developments and properties are described here.

2.1.1 Inorganic

Like conventional silicon electronics, metals and their alloys serve as the inorganic conducting materials in bioresorbable electronics [27]. Unique to metallic materials are the delocalized electrons that attribute to high thermal and electrical conductivities, low resistivities, and opacity to visible light [10, 107]. Electron mobilities exhibited by elemental metals are generally near 10 $cm^2/V{\cdot}s$ [107]. Furthermore, metals have high packing densities of atoms relative to other material types resulting in multiple slip planes attributing to exhibited notable ductility and strength [107]. Dissolvable metals used in bioresorbable electronics have low electrical resistance, predictable properties, and are biocompatible. The commonly employed metals in transient electronics include Mg, iron (Fe), zinc (Zn), molybdenum (Mo), and tungsten (W); each of which have inherent physiologic roles with the exception of W [14]. The metal alloy, AZ31B combines aluminum (Al) and Zn with trace amounts of other elements, and has been used in construction of a bioresrobable battery [27, 34, 116, 119].

Upon hydrolysis of the aforementioned metals, products formed include respective metal ions, oxides, or hydroxides [119]. Corrosion of the metals is driven by changing to a state that exhibits a lower Gibbs free energy Gibbs (G). The change in Gibbs free energy is directly related to the standard electrode potential through the relationship (Eq. 2) [119]:

Table 1 Key device components, common constituent materials, and corresponding reported dissolution behaviors

Device component	Purpose	Material	Dissolution mechanism	Dissolution conditions	Dissolution rate (nm/hr)[a]
Conductor	To transfer charge, commonly used in conductive components, like electrodes, interconnects, and antenna wires	Mg	$Mg + 2H_2O \rightleftharpoons Mg(OH)_2 + H_2$	SBF, 37 °C, pH 7.4	0.05–500
		Fe	$Fe + 2H_2O \rightleftharpoons Fe(OH)_2 + H_2$	SBF, 37 °C, pH 7.4	~2
		Zn	$Zn + 2H_2O \rightleftharpoons Zn(OH)_2 + H_2$	In vivo PBS	5
		Mo	$2Mo + 2H_2O + 3O_2 \rightleftharpoons 2H_2MoO_4$	Hank's solution, 37 °C, pH 7.4	0.3–1.1
		W	$2W + 2H_2O + 3O_2 \rightleftharpoons 2H_2WO_4$	In vivo	11.4
Semiconductor	Functions to manage charge flow and directionality; commonly found in transistors and diodes	Mono-Si (p-and n- type (10^{17} cm^{-3}))	$Si + 4H_2O \rightleftharpoons Si(OH)_4 + 2H_2$	0.1 M buffer solution, 37 °C, pH 7.4	0.132
		Mono-Si (p-type 10^{20} cm^{-3})	$Si + 4H_2O \rightleftharpoons Si(OH)_4 + 2H_2$	0.1 M buffer solution, 37 °C, pH 7.4	0.010
		Mono-Si (n-type 10^{20} cm^{-3})	$Si + 4H_2O \rightleftharpoons Si(OH)_4 + 2H_2$	0.1 M buffer solution, 37 °C, pH 7.4	0.021
		Mono-Si	$Si + 4H_2O \rightleftharpoons Si(OH)_4 + 2H_2$	Bovine serum	4.2
		a-Si	$Si + 4H_2O \rightleftharpoons Si(OH)_4 + 2H_2$	Buffer solution, 37 °C, pH 7.4	0.17
		p-Si	$Si + 4H_2O \rightleftharpoons Si(OH)_4 + 2H_2$	Buffer solution, 37 °C, pH 7.4	0.14
		Ge	$Ge + O_2 + H_2O \rightleftharpoons H_2GeO_3$	Buffer solution, 37 °C, pH 7.4	0.13

(continued)

Table 1 (continued)

Device component	Purpose	Material	Dissolution mechanism	Dissolution conditions	Dissolution rate (nm/hr)[a]
		SiGe	–	Buffer solution, 37 °C, pH 7.4	4×10^{-3}
		ZnO	$ZnO + H_2O \rightleftharpoons Zn(OH)_2$	DI H_2O, RT	13.3
Dielectric	Can aid in transferring charge to other device components, store charge and redistribute charge, and insulate electrical materials	SiO_2 (PECVD)	$SiO_2 + 2H_2O \leftrightharpoons Si(OH)_4$	Buffer solution, 37 °C, pH 7.4	–[b]
		SiO_2 (e-beam)	$SiO_2 + 2H_2O \leftrightharpoons Si(OH)_4$	Buffer solution, 37 °C, pH 7.4	–[b]
		SiO_2 (thermal)	$SiO_2 + 2H_2O \leftrightharpoons Si(OH)_4$	Buffer solution, 37 °C, pH 7.4	–[b]
		Si_3N_4 (LPCVD)	$Si_3N_4 + 12H_2O \rightleftharpoons 9Si(OH)_4 + 4NH_3$	Buffer solution, 37 °C, pH 7.4	–[b]
		Si_3N_4 (PECVD-LF)	$Si_3N_4 + 12H_2O \rightleftharpoons 9Si(OH)_4 + 4NH_3$	Buffer solution, 37 °C, pH 7.4	–[b]
		Si_3N_4 (PECVD—HF)	$Si_3N_4 + 12H_2O \rightleftharpoons 9Si(OH)_4 + 4NH_3$	Buffer solution, 37 °C, pH 7.4	–[b]
		MgO	$MgO + H_2O \rightleftharpoons Mg(OH)_2$	–	–
Substrate	Provides a foundation for functional components	Mg foil	$Mg + 2H_2O \rightleftharpoons Mg(OH)_2 + H_2$	aCSF, 37 °C	~167
		Fe foil	$Fe + 2H_2O \rightleftharpoons Fe(OH)_2 + H_2$	PBS, 37 °C, pH 7.4	3
		Zn foil	$Zn + 2H_2O \rightleftharpoons Zn(OH)_2 + H_2$	PBS, 37 °C, pH 7.4	14.5
		Mo foil	$2Mo + 2H_2O + 3O_2 \rightleftharpoons 2H_2MoO_4$	PBS, 37 °C, pH 7.4	0.8

Device component	Purpose	Material	Dissolution mechanism	Dissolution conditions	Dissolution rate (nm/hr)[a]
		W foil	$2W + 2H_2O + 3O_2 \rightleftharpoons 2H_2WO_4$	PBS, 37 °C, pH 7.4	6.25
		Silk	Enzymatic degradation	–	–[c]
		Cellulose derivatives	Dissolves in water	–	–
		POC	Hydrolysis of ester bonds	–	–
		POMC	Hydrolysis of ester bonds	–	–
		PLGA	Hydrolysis of ester bonds, enzymatic degradation	–	–
		PLA	Hydrolysis of ester bonds, enzymatic degradation	–	–
		PVA	Dissolves in water	–	–
		PGS	Hydrolysis of ester bonds, enzymatic degradation	–	–
Encapsulation	Serves as packaging, or encapsulating layers, to enhance mechanical robustness, protect device components, and prolong operational lifetime of the device	–[d]	–	–	–

Adapted under CC BY 4.0 License [79] and adapted with permission from Yin et al. [116]. Copyright 2014 John Wiley and Sons [10, 39, 49, 55–57, 9178, 93107, 119, 124, 125]

[a]Please note that degradation rates are reported from different study designs and cannot be compared directly; however, provided rates may instead be used as a general guide for dissolution trends. The affects of intrinsic and extrinsic factors on dissolution rates are reviewed in the text (Sect. 2)

[b]Only relative rates, not absolute rates, are reported for respective conditions [55]

[c]Complete dissolution of polymeric substrate films occurs on the order of minutes to years depending on processing conditions and environmental factors (Sect. 2.4.2)

[d]The common materials used for encapsulation are also used in other device components provided in the table (i.e., mono-Si, SiO_2, Si_3N_4, polymeric substrate materials) (Sect. 2.5)

$$\Delta G^{\circ} = -nFE^{\circ}, \tag{2}$$

where $\Delta G°$ is the change in the standard Gibbs free energy, n is the number of electrons transferred in the reaction, F is the Faraday's constant (96,486 J·(V·mol)$^{-1}$), and E° is the standard electrode potential in volts (V) [10, 119]. The electrode potential of metals are compared to the standard hydrogen electrode—an arbitrarily selected control cell for oxidation-reduction potentials with an understood E° of 0 V at 25 °C. Metals with higher reactivity than that of hydrogen in aqueous media are appealing candidates for metals in bioresorbable electronics for reliable dissolution in aqueous media [119]. Under nonstandard conditions, the electrode potential is calculated using the Nernst equation (Eq. 3) [119]:

$$E = E^{\circ} - \frac{RT}{nF}\ln(Q), \tag{3}$$

where E is the nonstandard electrochemical potential, R is the universal gas constant (8.314 J (mol·K)$^{-1}$), T is temperature in Kelvin, and Q is the reaction quotient determined from concentrations of the product and reagent ions [10, 119]. Using the electrode potential, Pourbaix diagrams can be constructed to determine the equilibrium state of each metal (i.e., metal, metal oxide) as a function of pH [119].

It should be noted that metals used in transient electronics are in thin film form consequently leading to possible variations in dissolution properties from the bulk material of the same metal [116]. Unlike bulk materials, defects in the material, such as pin holes, as well as grain size, will dramatically affect the rate of dissolution of thin films [15]. Furthermore, the dissolution of each metal in water or biofluids occurs at variable rates dependent on several intrinsic and extrinsic factors. Intrinsic factors correspond to the material itself. Examples include reactivity, surface chemistry, crystalline structure, microstructures, porosities, defects, and metal thickness. For example, the metal oxides that form upon corrosion are typically less soluble in water and degrade at slower rates than the parent metal in aqueous solution [78]. Extrinsic factors are dependent on the surrounding environment including solution pH, surrounding temperature, ion and protein concentration, O_2 levels, and processing conditions [27, 78, 116, 119]. Chloride ions in biological fluids expedite dissoltuion rates of some metals, such as Mg, by reacting with the parent metals or hydroxides to produce a metal chloride and hydrogen gas relative to environments with little to no chloride content [77]. Mg, Zn, and respective oxides dissociate more rapidly and in a less controlled manner than materials composed of Mo, Fe, W, and their oxides in aqueous solutions, which can help guide materials selection when considering the required functional lifetime of the medical device being fabricated [14, 27, 116, 119].

Magnesium Mg is the fourth most common mineral in the human body with highest abundance in skeletal tissue and intracellular fluid [24, 110]. This trace element activates over 600 enzymes with indispensable roles in calcium and phosphate

homeostasis, activation of cell metabolism, regulation of intracellular antioxidants, and stabilization of nucleic acids [24, 110].

To satisfy functional lifetime requirements of biomedical devices, it is crucial to assess the dissolution rates of bioresorbable materials. The standard electrode potential of Mg is −2.363 V, which is lowered, as expected, by the formation of surface hydroxide layers in aqueous media indicating the reduction of dissolution of the hydroxide species in water [10, 114, 119]. Due to high conductivity, existence in conventional electronics, established biocompatibility, and high dissolution rates, Mg was chosen as the conductive material in the first completely soluble silicon-based bioelectronic device [36, 117] [27]. In this device, Mg was incorporated into the inductor, capacitor, transistor, interconnects, and resistor pieces [36]. Upon dissolution, the hydroxide of Mg, $Mg(OH)_2$, is formed (Eq. 4) [116, 119]:

$$\mathrm{Mg} + 2\mathrm{H_2O} \rightleftharpoons \mathrm{Mg}\left(OH\right)_2 + \mathrm{H_2}. \tag{4}$$

Thereafter, in body fluids, $Mg(OH)_2$ will further react with chlorine ions to form the highly soluble salt, $MgCl_2$ [35]. Despite the formation of oxide and hydroxide features at the surface, the film thickness of Mg thin films has been shown to decrease linearly with time at rates dependent on the initial thickness of the film [77, 114, 116] with a reported weight loss rate of 19–44 mg/cm^2/day in Hank's solution (pH 6, 37 ˚C) as well as a surface area normalized dissolution rate of 0.05–0.5 μm per hour in simulated body fluid (SBF)under physiologic conditions (i.e., pH 7.4 and 37 °C) [98, 116]. The reported electrical dissolution rate (EDR)was higher than the mass loss dissolution rate for Mg at 4.8 ± 2.2 μm/hour in Hank's solution [117]. Aluminum (Al) can be added to Mg to reduce the dissolution rate [116]. Similarly, the Mg alloy, AZ31B, has a reduced EDR in Hank's solution of 2.6 ± 2.1 μm/hour [116]. Other magnesium films have incorporated silicon carbide (SiC), silicon dioxide (SiO_2), and polycaprolactone (PCL) to slow the dissolution of Mg as well [35]. Aside from alloying, Mg dissolution rates can be altered with distinct processing methods and/or coating layers [114].

Iron Over 60% of Fe is bound to hemoglobin present in red blood cells for delivery of oxygen, to body tissues while roughly 25% is stored until needed [43], and the remaining amount is predominantly bound to myoglobin in muscle cells or serves as a cofactor for enzymes needed for cellular function.

Fe has a positive $E°$ of +0.800 V signifying it is less readily soluble in water than Mg. When Fe thin films are immersed in water, the hydroxide by-product, $Fe(OH)_2$, results (Eq. 5) [116, 119]:

$$Fe + 2\mathrm{H_2O} \rightleftharpoons Fe\left(OH\right)_2 + \mathrm{H_2}. \tag{5}$$

In simulated body fluid at physiological conditions, Fe has a reported corrosion rate of 0.02 μm/hour [116]. The reported EDR of Fe in Hank's solution at pH 7.4 and 37 °C is 7×10^{-3} μm/hour, much lower than that of Mg in similar conditions [116].

Zinc Zn is a trace element with structural roles in protein folding and serves as a regulatory mediator in synaptic signaling, apoptosis, gene regulation, and catalysis [45]. Zn is a cofactor to over 70 enzymes, has antioxidant properties, and stabilizes endothelial membranes making it useful in the prevention of atherogenesis in cardiovascular stents and tissue scaffolds [8, 45].

The degradation products of Zn in aqueous solution include zinc hydroxide ($Zn(OH)_2$) and hydrogen gas (Eq. 6) [116, 119]. Further characterization has revealed that wires also break down into ZnO and Zn carbonate ($ZnCO_3$) in vivo [8].

$$Zn + 2H_2O \rightleftharpoons Zn(OH)_2 + H_2. \tag{6}$$

Zn degrades more slowly than Mg in body fluid and has an $E°$ of −0.763 V [10, 35]. Zn wire abdominal aorta stents reveal that Zn wires undergo uniform corrosion in rats for 3 months followed by localized, rapid corrosion behavior after 4.5 months with a corrosion rate ranging from 12 to 50 μm per year over the first sixth months [8, 35]. Another study reported an in vivo stent mass loss dissolution rate of 5×10^{-3} μm per hour [116]. The reported EDR was found to be 0.3 ± 0.2 μm per hour in Hanks' solution [116]. In regard to processability, Zn has a higher stability in organic solvents than Mg, which is more desirable for low-cost solution-based printing [35].

Molybdenum Mo is known to serve as a cofactor for various oxidases and catabolize sulfur-containing amino acids and heterocyclic compounds [35, 44, 109]. The dissolution of Mo results in the formation of molybdic(VI) acid (H_2MoO_4) (Eq. 7) [116, 119]:

$$2Mo + 2H_2O + 3O_2 \rightleftharpoons 2H_2MoO_4. \tag{7}$$

The $E°$ of Mo is −0.2 V. Unlike other bioresorbable metals, the EDR of Mo did not rise in acidic environments compared to that in water supported by an observed positive rise in $E°$ with increasing hydrochloric acid (HCl) concentrations [27, 99, 111]. Conversely, the solubility of Mo will increase with oxygen and chloride content [27, 35, 116]. The EDR of Mo under physiologic conditions is reported to be approximately $7 \pm 4 \times 10^{-4}$ μm/hour in Hanks solution (pH 7.4, 37 °C) [116].

Tungsten In contrast to the other metals used in bioresorbable electronics, W is not inherently found in the body; however, W thin films successfully deteriorate in aqueous solutions without eliciting toxic effects in vivo at concentrations less than 50 μg/mL [15, 116]. The hydrolysis of W produces tungstic(VI) acid (H_2WO_4) (Eq. 8) [116, 119]:

$$2W + 2H_2O + 3O_2 \rightleftharpoons 2H_2WO_4. \tag{8}$$

W has a $E°$ of +0.1 V and a dissolution rate that increases with pH. Furthermore, W deposited via chemical vapor deposition (CVD) dissolves at a rate that is an order of magnitude slower than W that is sputtered [27, 111]. CVD-deposited W had a reported EDR of approximately 2×10^{-3} μm/hour at physiological conditions, while sputter-deposited W had a determined EDR and mass loss corrosion rate of 0.02 μm/hour and 0.02–0.06 μm/hour, respectively [116].

2.1.2 Organic

Conjugated carbon systems support movement of delocalized electrons through a material and are therefore critical to conductive polymers [107]. Unlike inorganic conducting materials, besides electronic conduction, organic conductive materials are also capable of ionic conductivity, a common conduction pathway in the body involving the motion of ions through a material upon an applied electric field [47, 107]. Furthermore, electronic materials constituted of organic and carbon-based components (i.e., graphene and carbon nanotubes (CNTs)) have easily modified surface chemistries, can be designed to be flexible, and can undergo more economical manufacturing methods (i.e., solution processing) than conventional silicon electronics [119]. To date, main limitations include incompatibility with the conventional electronic fabrication methods with established manufacturing plants as well as inferior performance compared to metallic electrodes [119]. Scalable manufacturing methods and increasing conductivity of polymers to be comparable to that of metals for use in bioresorbable electronics are an area of ongoing research [22, 119].

One of the first organic electronic devices used melanin as the conductive component to make a resistive switching element, and more recently a derivative, eumelanin, has been used in biodegradable supercapacitors for energy storage [47, 68]. Another biodegradable organic material capable of conduction is chitosan, the deacetylated form of chitin, a material found in the exoskeleton of arthropods and in the cell wall of mushrooms [20, 47]. Chitosan thin films have been successfully fabricated on paper substrates [47]. Biocompatible, conductive polymers include polyaniline (PANI), polypyrrole (PPY), and poly(thiophenes) like poly(3,4-ethylenedioxythiophene) (PEDOT) and PEDOT-doped polyanion poly(styrene sulfonate) (PEDOT:PSS) [47, 119]. In PEDOT:PSS, PEDOT exhibits anionic conduction, while PSS facilitates movement of cations, like calcium (Ca^{2+}), sodium (Na^{+}), potassium (K^{+}), and acetylcholine (ACh) [47]. PEDOT nanotubes have been used for neural recording and PEDOT:PSS for in vivo biosensing and for high-performance electrodes in electrocorticography (ECoG) [35, 47].

Carbon based materials (i.e., graphene and carbon nanotubes (CNTs)) have found useful as conductive materials with graphene having reported electron mobilities as high as 200,000 $cm^2/V \cdot s$ [70, 107]. Oxidation of carbon nanotubes (CNTs), tubular structures of graphene, results in carboxylation of the surface facilitating degradation via oxidative enzymes [35]. Silkworms can be fed CNTs and graphene to create a conductive silk composite with improved mechanical strength due to

reinforcement from the carbon-based features [35, 120]. Graphene has been used as the conductive component in gelatin-based transient energy harvesters [70, 107].

2.2 Semiconductor

Semiconductors have intermediate conductivity between conductors and insulators [10, 49, 107]. To augment movement of charge carriers through *intrinsic* semiconductors, impurities coined *dopants* are added through a process called *doping* to alter the material into what are considered *extrinsic* semiconductors [10, 49]. Extrinsic semiconductors with electron-rich impurities, or donors, are referred to as n-type semiconductors, whereas p-type semiconductors are created by the addition of electron accepting dopants known as acceptors. Common examples of donor and acceptor impurities are phosphorous and boron, respectively [49]. Semiconducting materials are employed in transistors and diodes, namely, to govern charge flow and directionality [49].

2.2.1 Inorganic

Biocompatible semiconductors inlcude Si-NMs (i.e., polycrystalline (poly-Si), amorphous (a-Si), nanoporous (np-Si), and monocrystalline (mono-Si)), silicon-germanium (SiGe), germanium (Ge), and ZnO [18, 35, 39, 57]. Amorphous silicon (a-Si) and polycrystalline silicon (p-Si) can be found in solar cells and in the active matrix of flat panel displays, while SiGe is implemented in communication devices as well as high-frequency heterojunction bipolar transistors [57]. ZnO is a direct wide bandgap semiconductor (3.37 eV) that serves as a semiconductor in thin-film transistors and photodetectors. Furthermore, having optical transparency, high electron mobility, and piezoelectric properties, ZnO is a desirable material for mechanical energy harvesters and actuators [39, 50, 55]. Electronic mobilities for conventional inorganic semiconductors can vary between 1 $cm^2/V{\cdot}s$ to the order of 10^4 $cm^2/V{\cdot}s$ [107]. The dissolution reactions of each of these semiconducting materials lead to hydroxide or oxide products (Eqs. 9, 10, and 11) [119]. Currently, the most commonly used semiconducting material in bioresorbable electronics is Si as it is fundamental to conventional electronics with robust performance and an established biocompatibility profile [40, 59].

Orthosilicic (silicic) acid ($Si(OH)_4$), the by-product of Si hydrolysis, is a naturally occurring compound in the body with concentrations ranging from 14×10^{-6} to 39×10^{-6} M in serum [35, 59]. Silicon dissolves in a spatially uniform manner exhibiting linear kinetics indicating surface erosion rather than reactive diffusion with water [40, 59].

$$Si + 4H_2O \rightleftharpoons Si(OH)_4 + 2H_2, \tag{9}$$

$$Ge + O_2 + H_2O \rightleftharpoons H_2GeO_3, \tag{10}$$

$$ZnO + H_2O \rightleftharpoons Zn(OH)_2. \tag{11}$$

Environmental and intrinsic parameters can be used to tune degradation of semiconductors in order to meet lifetime requirements of desired bioresorbable devices. The dissolution rate of each of material is accelerated with temperature, which may be prevalent in the case of fever, local injury, or immune reactions [55]. Ge in buffer solution at physiological conditions dissolves at 3.1 nm/day—similar to mono-Si-NM—and will increase drastically with increasing pH. SiGe appears resistant to changes until a pH of 8, and deteriorates about 30 times slower than mono-SiNM (buffer solution, pH 7.4, 36 °C) [55, 79]. Although relatively resistant to changes in pH, SiGe dissolutions increase by approximately 185 times when placed into bovine serum compared to PBS at 37 °C, whereas Si degradation rates only increase 30–40 times under the same conditions [55]. Dissolution rates of mono-SiNMs can vary from 0.5 to 624 nm/day depending on surface chemistry, doping type and levels, temperature, and ion concentration in the surrounding solution, allowing for nanomembranes of silicon to disappear in a matter of days to weeks [35, 40, 59, 78]. The dissolution rate of Si-NMs increases with temperature and ion concentrations in aqueous solution (i.e., Ca^{2+} and PO_4^-), and exponentially, with pH as silicic acid, formation is catalyzed by hydroxyl ions [35, 119]. Conversely, dissolution rates of Si are decreased by doping levels that exceed 10^{20} cm^{-3}, the presence of silicic acid in solution, and proteins in solution [59, 74]. When in similar conditions (buffer solution at 37 °C and pH 7.4), the morphology of Si alone can affect dissolution rates where a-Si degrades faster rate than p-Si, due to enhanced diffusion, followed by mono-SiNM [59, 79]. For ZnO, a 20 nm-thick film fully dissolves at room temperature in deionized (DI) water in 15 hours [119].

2.2.2 Organic

Biodegradable organic semiconducting compounds have conjugated carbon systems like in conducting polymers. Examples include β-carotene, indigo, perylenediimide (PDI), chlorophyll, and derivatives of anthraquinone, indanthrene brilliant orange RF, and indanthrene yellow G [35]. Appealing attributes of organic as opposed to inorganic semiconductors include low-cost, high-throughput low-temperature fabrication techniques (i.e., large-area, solution-based processing), high mechanical flexibility, and diverse surface functionalization [59, 76].

Unfortunately, however, many natural, organic semiconductors used in transient electronics exhibit intrinsically low carrier mobilities compared to traditional semiconducting materials used in currently fabricated transient electronic devices, which is a limitation for facilitating interfacial charge transport [22, 46, 59]. Mono-Si typically exhibits an electron mobility of 1400 $cm^2 \cdot (V \cdot s)^{-1}$, whereas β-carotene and indigo have much lower mobilities (4×10^{-4} $cm^2/(V \cdot s)$ and 1×10^{-2} $cm^2/(V \cdot s)$,

respectively) [35, 48, 59]. Diketopyrrolopyrrole (DPP)can be conjugated with p-phylenediamine (PPD) to synthesize the bioresorbable, semiconducting polymer, PDPP-PD. Degradation begins initially degrading by acid catalysis of the imine bonds followed by hydrolysis of the lactam group present in the DPP monomers [59, 76]. PDPP-PD exhibited a carrier mobility as high as 0.21 ± 0.03 $cm^2/(V \cdot s)$ when used with an aluminum oxide (Al_2O_3) dielectric, gold (Au) electrodes and gate, and cellulose substrate [59].

Other organic compounds investigated as biodegradable semiconductors include perylenediimide (PDI), a chromophore for red cosmetics, used in an edible OFET, and 5,5′-bis(7-dodecyl-9*H*-fluoren-2-yl)-2,20-bithiophene (DDFTTF) explored to assemble OTFTs made with a poly(vinyl alcohol) (PVA) dielectric, Au and silver (Ag) electrodes, and poly(lactic-co-glycolic acid) (PLGA) substrate to accomplish carrier mobilities of ~0.25 $cm^2/(V \cdot s)^{-1}$ [5, 46]. Electron mobilities for existing polymer semiconductors can extend up to 10 $cm^2/(V \cdot s)$ [107]. Translating higher mobilities exhibited by conventional organic materials to safe and practical organic semiconductors for bioresorbable devices is an area of research that necessitates further exploration.

2.3 Insulator: Dielectric

In capacitors, dielectric materials store and transport electrical charge and/or can be used to isolate an electrical charge from the surrounding components in electronic devices [10, 107]. Higher dielectric constants in parallel plate capacitors signify an increase capacitance for a given area [10]. In bioresorbable electronics, gate and interlayer dielectrics as well as passivation coatings are comprised of dielectric materials [55, 119]. Moreover, thin film dielectric materials mitigate short circuiting and are resistant to water penetration making them especially instrumental in hydrolytic protection (Sect. 2.5) [55].

2.3.1 Inorganic

Inorganic biocompatible and biodegradable dielectric materials include SiO_2, MgO, silicon nitride (Si_3N_4) magnesium fluoride (MgF_2), and spin on glass (SOG) [48, 56, 59, 78, 121]. SiO_2 and Si_3N_4 are widely adopted dielectric materials in current microelectronics. Amorphous SiO_2 has a dielectric constant of 3.9 at 1 MHz with high electrical resistivities making it a suitable material for insulation and passivation [35, 107]. Si_3N_4 exhibits a high dielectric constant of around 7 and has been used as the gate dielectric in TFTs and for charge storage in nonvolatile memory devices in microelectronics [35, 94]. MgO is commonly utilized as a gate dielectric in transistors and as the dielectric layer in capacitors [35]. Thin-film MgO exhibits optical transparency, high electrical resistivity, chemical and thermal stability, and high dielectric permittivity values ranging from 8 to 10 depending on temperature and

frequency, with a dielectric constant of 9.65 at 1 MHz [107, 119]. MgF_2 has a band-gap of 11.3 eV and a dielectric constant ranging from 4.87–5.45 at 1 MHz. MgF_2 is the dielectric material in the bioresorbable resistive random-access memory (RRAM) device for memory storage developed by Zhang et al. [121, 123].

The dissolution reaction for SiO_2 yields silicic acid ($Si(OH)_4$) as a by-product (Eq. 12) [55]:

$$SiO_2 + 2H_2O \leftrightharpoons Si(OH)_4. \tag{12}$$

After a two-step dissolution reaction of Si_3N_4 (Eqs. 13 and 14), the net products are $Si(OH)_4$ and ammonia (NH_3) (Eq. 15) [55]:

$$Si_3N_4 + 6H_2O \rightleftharpoons 3SiO_2 + 4NH_3, \tag{13}$$

$$SiO_2 + 2H_2O \rightleftharpoons 3Si(OH)_4, \tag{14}$$

$$Si_3N_4 + 12H_2O \rightleftharpoons 9Si(OH)_4 + 4NH_3. \tag{15}$$

The dissolution kinetics of dielectric materials are affected by the morphology, density, and chemical stoichiometry [59]. The type of deposition process can control the density of a dielectric film. Kang et al. studied the dissolution behaviors of SiO_2 grown by wet and dry thermal growth with oxygen gas and water vapor, respectively, plasma-enhanced chemical vapor deposition (PECVD), and electron beam (e-beam) deposition in buffer solutions between pH 7.4 and 12 at room temperature as well as at 37 °C. In the same study, dissolution behavior of Si_3N_4 deposited by low-pressure chemical vapor deposition (LPCVD), low-frequency PECVD (PECVD-LF), and high-frequency PECVD (PECVD-HF) was investigated at the same pH range and temperatures as SiO_2 [55]. Dissolution rates were determined by ellipsometry and atomic force microscopy to evaluate surface topography changes with dissolution over time [55]. It was found the dissolution rates of SiO_2 under the same conditions were fastest when grown via e-beam deposition and slowest through thermal growth consistent with e-beam deposition exhibiting fragmentation and having lowest densities and highest diffusivities relative to PEVCD-deposited materials and thermally grown materials that yield the most dense and uniform growth of the three methods [55]. The LPCVD-deposited Si_3N_4 possessed the highest density and lowest dissolution rate, followed by the PECVD-LF-deposited Si_3N_4, and PECVD-HF-deposited Si_3N_4 which had the lowest density and the highest dissolution rate [55]. The dissolution was uniform for each type of growth process, and the dissolution rates increased in bovine serum compared to buffer solution along with temperature, ion concentration, and pH as hydroxyl ions (OH^-) are understood to initiate the dissolution reaction [55].

In the dissolution of MgO, the dissolution yields a $Mg(OH)_2$ by-product (Eq. 16) [35]:

$$MgO + H_2O \rightleftharpoons Mg(OH)_2. \quad (16)$$

The dissolution rate of MgO trends inversely with pH as the reaction is driven by protons (H^+) [21, 35]. MgO was determined to have a morphological dissolution rate of 50 nm per hour in deionized water at room temperature [119].

2.3.2 Organic

Most bioresorbable devices investigated used inorganic dielectric materials; however, various organic molecules have been explored as dielectric materials in transient transistors, energy storage devices, and pressure sensors. Organic materials investigated span from nucleotides, polysaccharides, caffeine, and egg albumen to silk fibroin, keratin, and gelatin along with synthetic and flexible polymers, such as poly(vinyl alcohol) (PVA), poly(glycerol sebacate) (PGS), and poly(lactic-co-glycolic acid) (PLGA) [14, 33, 35, 59, 65, 79, 105, 113, 119]. At 1 kHz, dielectric constants of these organic semiconductors range from ~3.85 to ~7.6 [46].

2.4 Insulator: Substrate

The substrate serves as the foundational supporting material for the electrical components during processing, handling, and/or operation. In bioresorbable electronics, biodegradable polymers typically serve as the substrate material. In response to low thermal stability, water permeability, and sensitivity to standard IC photolithography and etching fabrication methods of most biodegradable polymers, metallic foils and bioactive glasses have been realized to overcome this limitation [14, 22, 56]. Substrate layers typically have a thickness on the order of microns and can be engineered to fully degrade at rates from almost instantly to over several years [22, 63, 119]. Many substrate materials also function as encapsulation layers and dielectrics in transient devices [119].

2.4.1 Inorganic

Metallic substrates are mechanically robust with high dimensional stability compared to biodegradable polymeric substrates that are sensitive to standard electronic fabrication techniques and swell in solution [56, 78]. Metal foils with a thickness of ~10 μm exhibit low bending stiffness while retaining mechanical toughness and reasonable dissolution times for bioresorbable electronics [56]. Metal thin foils of biocompatible metals (Fe, Mo, Zn, W, and Mg) have served as substrates in n-channel metal-oxide-semiconductor field-effect transistors (n-MOSFETs), Si PIN diodes, capacitors, and inductors.

Degradation rates of the thin metal foils vary depending on thickness of the foil, grain morphology, and surface structure as well as solution temperature and composition [14, 56, 119]. Metal thin foils without a SiO_2 coating were submerged into solution under various degradation conditions. In PBS solution (pH 7.4 and 37 °C), the Mo and Fe foils exhibited similar rates of dissolution (0.02 and 0.08 μm/day, respectively) with W having a slightly faster rate (0.15 μm/day) followed by Zn foils (3.5 μm/day) [56]. When used in a bioresorbable electronic brain sensor, the Mg foil was found to degrade at a high rate of 4 μm/day in artificial cerebrospinal fluid (ACSF)at 37 °C [58]. Contrary to metal thin films, Mo and Fe metal foils dissolve faster in Hank's solution compared to PBS. This conflicting behavior was attributed to morphology differences of foils compared to thin films and possible differences in solutions between each study.

Adnan et al. developed a biodegradable borate bioactive glass that was completely soluble in simulated body fluids to use as a substrate for a spiral, thin film resistor, inductor, capacitor (RLC) resonator device [2]. Bioactive glasses have been used in tissue engineering and are considered safe in vivo. The intention to use a glass material as a substrate was to retain structural integrity without swelling or disintegrating to prolong lifetime of a transient electronic device while withstanding IC processes to enable direct fabrication [2]. The bare borate glass substrates were dissolved in simulated body fluid at 37 °C. Time to complete dissolution was about 40 hours having a dissolution rate of 5.5 mg/hour with a surface area of 4.35 cm^2 [2]. Although a borosilicate glass was tested for this study, the composition of the glass can be varied to acquire desired properties for device function [2]. Glasses primarily composed of silicate dissolve at a slower rate than borosilicate glasses, ranging from 10% weight loss per day to 50% weight loss per day, respectively [2]. Bioactive glasses can also contain calcium and sodium. In these cases, sodium dissolves into solution, while calcium binds to extracellular phosphates causing eventual formation of porous hydroxyapatite, a mineral found in native bone tissue [2], which may not be desirable for fully resorbable devices.

2.4.2 Organic

Organic substrates possess a wide range of properties, degradation products, and dissolution behaviors. Despite limitations in conventional electronic fabrication, polymer substrates are redeemed by tunable properties, ease of chemical functionalization, Food and Drug Administration (FDA) approval for biomedical uses, and benign and economical processing compared to that of metals [56]. The primary degradation mechanisms of current biodegradable polymers in the body occur through hydrolysis of carbonyl functional groups or enzymatic degradation [35]. Additional degradation mechanisms empoloyed by transient substrates include oxidation and UV radiation exposure [22].

Polymers with slow swelling rates are desirable to eschew premature device disintegration during dissolution [78]. Functional lifetime and corrosion behavior can be adjusted by altering composition, crystallinity, surface chemistry, and thickness

of the polymer. Hydrophilic polymers undergo accelerated dissolution in aqueous solutions compared to hydrophobic counterparts. Meanwhile, slower dissolution rates occur with increasing crystallinity [22, 35]. Degradation mechanisms of polymers can also affect dissolution rates. Namely, polymers that undergo dissolution, rather than biodegradation, frequently reveal faster transience. Surface erosion and enzymatic degradation typically transpire at slower rates compared to bulk degradation [22, 119].

Key organic substrates used in transient devices can be subdivided into *natural* organic materials and *synthetic* organic and carbon-based materials. Key natural materials reviewed herein are silk, cellulose, and cellulose ethers, and rice paper, and synthetic materials reviewed below include poly(lactic acid) (PLA), poly(glycolic acid) (PGA), poly(lactic-co-glycolic acid) (PLGA), polycaprolactone (PCL), poly(octamethylene citrate) (POC), poly(octamethylene maleate citrate) (POMC), poly(glycerol sebacate) (PGS), and poly(3-hydroxybutyrate-co-3-hydroxyvalerate) (PHB/V).

Natural Silk was used as the substrate in early partial and fully bioresorbable electronic devices [36, 62]. Silk originates from silk worms, being the strongest and toughest natural fiber known to date, with tunable optical and mechanical properties [105]. Silk isolated from the cocoons of silkworm larvae is composed of the proteins fibroin and sericin [14, 63, 119]. While sericin induces an inflammatory response in humans, silk fibroin is immunologically benign and is therefore purified from raw silk for use in bioimplant applications [105]. Silk fibroin has increased conformability to tissues with decreased thickness. Film thickness and crystallinity, tuned by controlling β-sheet formation, can control degradation times on the order of minutes to years along with mechanical properties [22, 119]. Main processing conditions of silk are mild occurring in water-based, neutral pH solutions at room temperature [105]. Silk has been processed into many forms including hydrogels, ultrathin films, thick films, conformal coatings, three-dimensional porous and solid matrices, and fibers for use in tissue engineering, wound dressings, surgical sutures, implantable devices, and drug delivery [14, 105, 119].

Another resilient polymer from nature is cellulose and cellulose-derived materials. Water soluble derivatives including methyl cellulose, sodium carboxymethyl cellulose (Na-CMC), and cellulose nanofibril paper, are natural, low-cost, and nontoxic insulating materials [27, 78]. Cellulose is the most abundant organic polymer on Earth composed of β-sheets of D-glucose monomers primarily found in the cell walls of plants serving as a structural material and is commonly sourced from tree bark [22, 101, 119]. Due to the high thermal and chemical stability of cellulose, it is possible to fabricate electronic devices onto cellulose substrates directly for potential roll-to-roll fabrication in addition to transfer printing methods used for other organic substrates with success in printed and paper-based electronics [22, 119]. Nanocellulose paper is a transparent material that can be used as a substrate and has been implemented into OFETs [27]. A water-soluble cellulose ether, methylcellulose, has been used for thermo-responsive transient electronics due to its low critical solution temperature (45 °C), while another cellulose ether, carboxymethyl cellu-

lose, has served as a substrate that can dissolve in water within 10 minutes for bioresorbable printed circuit boards, heterojunction bipolar transistors (HBTs), and screen and laser printed bioresorbable conductors [27, 119]. For enhanced flexibility and faster time to complete degradation compared to thicker films, cellulose films on the order of 800 nm have been created via functionalizing cellulose with trimethylsilyl groups with successive hydrolytic deprotection [22].

Rice paper is an alternative low-cost option for substrate materials [41, 78, 119]. However, rice paper swells rapidly upon contact with water, causing functional components of the device to rupture quickly thereby limiting its use. A CMOS inverter device using a rice paper film substrate with 200 μm thickness disintegrated within 48 hours in DI water at 37 °C [41]. Other natural substrate materials less commonly experimented with include hydrogels like alginate and gelatin, cheese and seaweed, sugar-based epoxy, and charcoal (i.e., an allotrope of carbon) used alone or synthesized with other polymers [35, 59, 119].

Synthetic Biodegradable aliphatic polyesters commonly used in US Food and Drug Administration (FDA)-approved medical devices include the poly(α-hydroxy) acids: PLA, PGA, PLGA, and PCL [14]. These and the elastomers, POC, POMC, PGS, and PHB/V, degrade primarily through hydrolysis of ester bonds in aqueous solution [6, 7, 14, 69, 93]. Degradation rates may vary with time in solution, molecular weight, and polymer composition [14]. The substrates composed of PLA, PLGA, PGA, PCL, and PHB/V, and others are commonly fabricated via spin casting, hot melting, and electrospinning [119].

PLA and the copolymer, PLGA, formed by the ring opening polymerization reaction of lactide and/or glycolide is amongst the most widely used commercially available polymers for biomedical use in pharmaceuticals, tissue engineering, and medical devices[14, 83]. The polymer is composed of lactic acid (LA) and/or glycolic acid (GA) units. The presence of the methyl moiety in lactic acid gives PLA higher crystallinity and hydrophobicity relative to PLGA resulting in longer degradation times at the tradeoff of flexibility compared to similar molecular weight PGA [78, 119]. Likewise, PLGAhas tunable degradation rates from weeks to months being prolonged by increasing LA content and molecular weight [14, 22, 27, 30]. Moreover, the enantiomers of lactic acid can be used to modify degradation rates of PLA or PLGA with the l-isomer yielding a higher crystalline polymer (PLLA) and degradation rates compared to similar molecular weight polymers composed of the racemic mixture of LA (PDLA) [14]. PLA and PLGA polymers are highly processable, being fabricated into forms like films, scaffolds, hydrogels, and micro- and nanospheres [14, 83].

Poly(caprolactone) is an aliphatic polyester comprised of hexanoate monomers synthesized by polycondensation of 6-hydroxyhexanoic acid or, more commonly, via the ring opening polymerization of ε-caprolactone [69]. PCL typically has a slower degradation rate and higher hydrophobicity relative to PLGA and PGA due to a high degree of crystallinity (up to 69%) [35, 69]. The mechanical properties of PCL including tensile strength, Young's modulus, and elongation at break range from 4 to 785 MPa, 0.21 to 0.44 GPa, and 20 to 1000%, respectively, due to varia-

tions in molecular weight, crystallinity, and dissolution environment, which also affect rate of degradation [69]. Additionally, copolymerization with other polymers like PLGA, PLA, and PGS leads to enhanced properties, such as shape memory, flexibility, and elasticity [35, 69, 88]. Besides hydrolytic cleavage, thermal stimulation can achieve transience in devices containing PCL. At temperatures higher than the melting temperature (60 °C), the polymer quickly wrinkles and shrinks in a matter seconds [29]. An applied voltage can induce heating in a transient device as by Gao and colleagues [29].

Polyhydroxyalkanoates, like PHB/V, are another type of polyester family formed by bacteria or through copolymerization; for example, the copolymerization of 3-hydroxybutanoic acid and 3-hydroxypentanoic acid produces PHB/V [126]. Polyhydroxyalkanoates are biocompatible and shown to have nontoxic byproducts after degradation via hydrolysis [95, 119]. Although 50 μm films of PHB/V were reported to fully degrade over 50 weeks in sea water at 15 °C, a device with an encapsulating layer made of PHB/V lasts tens of minutes once sweat covers the PHB/V and enters its surface [6].

In many circumstances, flexibility and elasticity of implantable materials are essential to fit to the curvilinear and dynamic anatomical structures in the body [22, 27]. In these cases, a lightly cross-linked network polymer with viscoelastic properties, or an *elastomer*, serves as an ideal insulator for substrate and encapsulating layers [27]. As mentioned above, POC, POMC, and PGS are three well-established elastomers employed in transient electronics [27, 35, 59, 78]. POC, a polymer composed of two nontoxic monomers (citric acid and 1,8-octanediol), is synthesized via a scalable, facile, one-pot polycondensation reaction without the use of catalysts [115]. POC has versatile and widely recognized use in tissue engineering and drug delivery [42, 115]. Similar to other synthetic polymers, the mechanical and degradation properties of POC can be finely tuned depending on monomer ratios, cross-linking conditions, molecular weight, compositing, and functionalization of the polymer [115]. The rate of dissolution is further altered by temperature, solute concentration, and pH of the dissolution media [27]. The Young's modulus for POC can range from 2.84 to 6.44 MPa, and the polymer has an elongation at break varying from 253% to 375% [35]. In PBS, at pH 10 at room temperature, POC degrades over several weeks [27]. Hwang et al. have used POC as a substrate and encapsulating material for CMOS MOSFET technology to create a electrocardiography monitor (EKG) and pH sensor [42]. The POC film used in this device could be stretched to roughly 30% [42].

Not only does POC have appealing degradation and mechanical properties, it can be easily formulated with other monomers creating a biodegradable, citrate-based material platform for versatile biomedical applications [100]. An example is the addition of the maleic anhydride to citric acid and 1,8-octane diol resulting in a photocross linkable elastomer, POMC, which has been used in an flexible, bioresorbable strain and pressure sensor for postsurgical tendon repair monitoring; meanwhile, the addition of amino acids, like cysteine and serine, manifests photoluminescent properties creating biodegradable photoluminescent polymers (BPLPs) for applications in bioimaging, drug delivery, and tissue engineering [85, 100].

Furthermore, BPLP has been successfully doped with aniline tetramer to synthesize electroactive, biodegradable elastomers that have controllable elasticity, conductivity, and degradation with dual-imaging capabilities [96]. To increase the mechanical strength of POC and BPLP, *hexamethylene diisocyanate* (HDI) can be reacted with each to result in cross-linked urethane-doped polyester (CUPE) and urethane-doped biodegradable photoluminescent polymers (UBPLPs), respectively [19, 85, 100].

PGS is another elastomer developed in 2002 by Wang et al. and is synthesized via the polycondensation reaction of glycerol and sebacic acid [6, 113]. PGS exhibits a Young's modulus ranging from 0.05 to 2 MPa and an elongation at break of greater than 260%. PGS has been used as a substrate in a piezoelectric pressure sensor device demonstrating no significant change in viscoelastic behavior after 7 weeks in PBS at 37 °C [6]. Like polyanhydrides, PGS undergoes surface erosion rather than bulk degradation as do the poly(α-hydroxy) acids, explaining a long functional lifetime [6, 14, 93, 119]. Only 17% of PGS was reported to degrade when incubated in agitated PBS at 37 °C for 60 days in vitro, while in vivo surface degradation revealed to be between 0.2 and 1.5 mm per month [6, 35].

Polyanhydrides are versatile, biocompatible copolymers of methyl vinyl and maleic anhydride groups that can be aliphatic, aromatic, or a mixture of both [31, 95]. Moreover, acrylated anhydrides capable of UV and visible light induced cross-linking have been designed to permit alternative processing regimes [95]. Polyanhydrides have been extensively studied in tissue engineering, medical devices, and controlled-release drug delivery [60, 95]. Polyanhydrides have reported tensile strengths of 25–27 MPa with a Young's modulus around 1.3 MPa and elongation at break between 14% and 85% [95]. To improve mechanical properties, polyanhydride can be copolymerized with polyimide as tried in orthopedic applications [95]. Polyanhydrides typically exhibit controlled surface erosion, rather than bulk degradation [31, 60, 119]. The degradation products, diacid and linear methacrylic acid molecules, of polyanhydrides, dissolve in water [95, 119]. The rates of degradation can be tuned from days to weeks in biofluids by increasing the degree of crystallinity and anhydride composition [28, 31, 95, 119]. Combination with poly(ethylene glycol) (PEG) has been reported to increase degradation rates [28, 53].

Substrate layers composed of poly(vinyl alcohol) PVA and poly(vinylpyrrolidone) (PVP) are nontoxic and water-soluble, demonstrating reversible dissolution occurring within minutes at room temperature at modifiable rates according to solution temperature and degree of polymerization [27, 54, 119]. These polymers are soluble in polar solvents allowing their use in printing inks, food products, pharmaceuticals, and cosmetics [27, 119]. PVA has been composited to adjust degradation rates and mechanical properties [1, 10]. PVA composites with gelatin and sucrose prolonged and expedited dissolution in water, respectively, compared to PVA alone. The decrease in the dissolution rate and swelling of the PVA/gelatin composite were attributed to collective hydrogen and ester bonding believed to form a stable, triple-helix structure, whereas the increase in the dissolution rate of the PVA/sucrose composite was rationalized by the high solubility of sucrose in water [1, 119].

2.5 *Insulator: Encapsulation Layer*

Encapsulation, or encapsulating, layers prolong lifetime in addition to increasing mechanical robustness of transient electronic devices. When using an encapsulating layer on a bioresorbable device, two-phase dissolution kinetics are classically observed with the initial dissolution of the encapsulation layer being slow followed by an expedited dissolution of the metal components resulting in rapid functional decline [36, 38, 56, 119]. This outer layer is critical to translatable bioresorbable electronics since electrical failure ensues once electronic materials come into contact with water, shortening the final lifetime before complete dissolution of the transient electronic components [119]. Typically swelling or nonuniform dissolution due to pinhole defects, pitting corrosion, or inconsistent composition is more pronounced in single-layer materials compared to bulk counterparts of substrate and encapsulating layers contributing to premature water diffusion of thin pieces in transient electronics. Recent developments to increase efficacy of encapsulating layers include compositing (Sect. 2.4.2), designing air pockets between semipermeable layers for indirect passivation between layers, and using various deposition techniques to reduce water permeable defects [1, 31, 55, 59, 78, 119]. Polymeric materials and film oxides like silk, polyanhydrides, PVA, PCL, PLGA, MgO, SiO_2, and Si_3N_4 are commonly used alone or in combination to form encapsulating layers with more recent investigation of p-type Si-NMs for this use [59, 74, 90, 119]. Novel encapsulation designs are of high interest as this layer provides a great opportunity to accomplish triggered degradation and precisely control functional lifetimes of transient devices [16, 36, 119].

2.5.1 Inorganic

The superior thermal and mechanical stability of inorganic materials relative to organic pieces inspires investigation of inorganic materials for protective coatings in bioresorbable electronics [35, 119]. In the first fully reported transient N-MOSFET device, a bilayer of MgO and highly crystalline silk protected the electrical components of the device for as much as 90 hours [36]. An 800 nm encapsulating layer of MgO alone on an inverter permitted protection against degradation for approximately 7 hours; meanwhile, in another study, a MgO layer (1–3 μm) provided a functional lifetime between 4 and 7 hours [39, 56]. A metal insulator metal (MIM) capacitor and Mg spiral inductor using metallic glass substrates were encapsulated with a 3 μm of layer of MgO and demonstrated stable operational times of approximately 5 and 6 hours in DI water at room temperature, respectively [56].

Recently, mono-Si-NM encapsulating layers (1.5 μm) have been studied for encapsulation for Mg thin films degrading at a rate of ~4.8 nm/day to keep the Mg film intact for over 60 days in PBS at 37 °C. In contrast, the same Mg film degrades within minutes using PLGA (5 μm) or e-beam-deposited SiO_2 (200 nm) encapsulating layers in PBS at room temperature. Boron-doped Si-NM encapsulating layers

degraded at rates of 1–60 nm per day depending on degradation conditions. Lifetime of Si-NM-protected Mo/Si electrodes is expected to be roughly 50 days at 37 °C [75].

Silicate-based SOGs are appealing for insulation, and encapsulation as SOGs have tunable dissolution rates in aqueous solution, demonstrated in vitro cytocompatibility, established use in conventional electronics, and provide deposition that is confroms tightly with its substrates. SOGs were cured at different temperatures to control dissolution rates ranging from 6 nm/day and 50 nm/day when cured at 800 °C and 300 °C, respectively (PBS, nitrogen purge, pH 7.4, 37 °C). Less Si-O-Si bridges that provide stability against hydrolysis form at the glass surface at low curing temperatures compared to high temperatures [56].

It was shown that dissolution times can be prolonged synergistically by depositing alternating layers of SiO_2 and Si_3N_4 by PECVD to minimize exposed defects [55]. Furthermore, uniform deposition methods (i.e., atomic layer deposition (ALD)) result in less defects than PECVD. Therefore, ALD can be used to coat PECVD-deposited materials to lengthen dissolution times compared to PECVD-deposited materials without ALD-deposited coatings [55].

2.5.2 Organic

Although not as mechanically or chemically durable compared to inorganic materials, organic encapsulation layers are useful in transient devices to provide flexibility and can increase device robustness by reducing stress accumulation at interconnects [58, 73]. Many of the same organic materials used as substrates and dielectrics are also used as the packaging materials. It should be considered that many organic polymers are permeable to water and can swell causing rapid deterioration of the functional device components [119]. Adjusting crystallinity, encapsulating layer thickness, degree of polymerization, and monomer ratios of constituent polymers, as well as compositing, can alter water resistance, swelling, and degradation time of polymeric encapsulating layers [17, 27, 78].

PLA was used as an encapsulating layer for a piezoelectric force sensor in a resorbable intra-organ pressure monitoring device that performed unchanged for up to 16 days in vivo [17]. In a study conducted by Tsang et al., PCL (5 μm) coated biodegradable iron/magnesium batteries resulted in battery performance of 30 μW of power for 100 hours. This was reported to be sufficient to operate low-power transient implants, such as pacemakers, low-power neurostimulators, or flow rate sensors, for a matter of days [108]. Polyanhydrides have also been used as an encapsulating layer in bioresorbable electronics due to their low permeability to water and surface erosion behavior to minimize swelling and resulting potential damage to electronic components [28, 58, 73]. An 120-μm-thick polyanhydride encapsulation layer permitted stable operation of an intracranial pressure (ICP) sensor in vivo for a maximum of 72 hours. Another hydrophobic polyanhydride was synthesized to encapsulate a bioresorbable microsupercapacitor (MSC), a small-scale energy storage device composed of metal electrodes and electrolyte hydrogel [58, 59]. Similarly, Lee and colleagues used a thick hydrophobic polyanhydride

encapsulation layer to protect MSC components while reducing water evaporation from the electrolyte solution and keeping it from contact with the surrounding media to prolong device lifetime compared to the use of a thinner PLGA encapsulating layer (Sect 3.1.3) [73]. Thermal sealing was used for PVA packaging of a transient lithium battery as well as for a multilayer silk encapsulated transient split-ring resonator antenna where noncrystalline silk layers coated the device and were then thermally sealed with an outer layer of crystalline silk [9, 26, 119]. The air pocket formed between the semipermeable crystalline and noncrystalline layers fills with water vapor instead of fluid to prolong diffusion of water through the encapsulating layer. Further increasing amount of silk layers and pockets lengthened time to device failure [9].

3 Applications in Biomedical Engineering

Through advancements in flexible electronics, deposition and fabrication techniques, degradable CMOS, wireless communication, and memory storage technologies, bioresorbable electronics have foreseeable potential for translation to biomedically relevant devices possessing complete transience, conformal contact to tissues, and enhanced precision relative to conventional diagnostic, treatment, and monitoring tools [14, 65, 79, 97, 121]. Application of transient electronic implant in clinical settings evades the necessity for a secondary removal procedure and potential complications while minimizing the risk for foreign body response, infection, device migration, and physical damage to surrounding tissue with essentially no e-waste production once the device is no longer needed [27]. Herein, key representative devices composed of materials previously discussed (Sect. 2) critical to advancing resorbable power sources, biosensing devices, and therapeutic systems are reported (Fig. 3). Table 2 provides a comprehensive reference guide to bioresorbable systems including and beyond the devices that are discussed in this section.

3.1 Energy Supply

A considerable restraint to realizing practical use of many transient devices is the need of external power sources for successful operation. Self-sustainable, wireless energy supplies are therefore crucial for the progression of transient electronics in order to function independently and extend operational lifetimes [81]. Representative examples of current energy sources include batteries, mechanical energy harvesters (MEHs), and microsupercapacitors (MSCs) [34]. Bioresorbable radiofrequency antennas and power scavengers have also been developed for wireless power and communication [119].

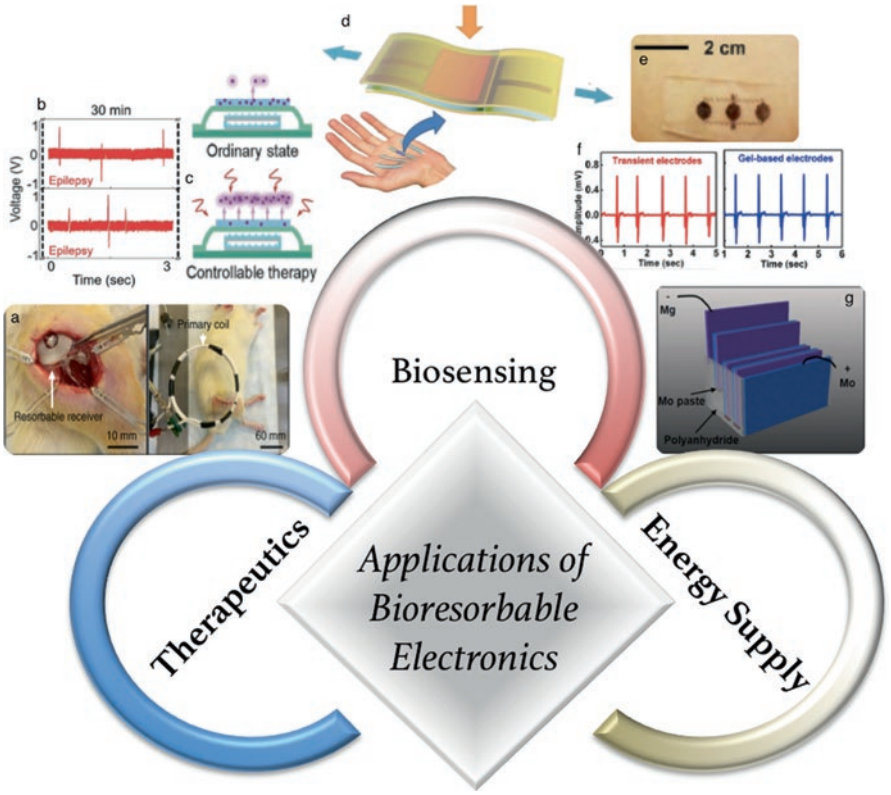

Fig. 3 Main classes and respective representative devices of clinically translatable bioresorbable electronics (**a**) Postoperative wireless stimulation by a bioresorbable device equipped with a radiofrequency power harvester connected to an electrical interface provided to a transected rat sciatic nerve for enhanced peripheral nerve regeneration. (Reprinted by permission from RightsLink Permissions Springer Nature Customer Service Centre GmbH: Springer Nature Nature Medicine [66] Copyright 2018). (**b–d**) A resorbable dual monitoring and treatment device powered by a triboelectric nanogenerator (TENG) for epilepsy management. (Adapted with permission from Zhang et al. [120]. Copyright 2018 John Wiley and Sons). (**b**) Detection by a drug-loaded device of epileptic signals (top) compared to an empty control (bottom) (**c**) A schematic of the inactive device (top) and activated device releasing drug due to resistor-mediated thermal stimuli triggered by epileptic signals (**d**) a dual-functioning, flexible pressure sensor and strain gauge foreseen to be used to guide patient-specific treatment for postoperative tendon repair. (Reprinted by permission from RightsLink Permissions Springer Nature Customer Service Centre GmbH: Springer Nature Nature Electronics [7]. Copyright 2018). (**e**, **f**) an electrophysiological (EP) sensor adhered to a POC substrate for EKG monitoring. (Adapted with permission from Hwang et al. [42]. Copyright 2015 American Chemical Society.) (**e**) The EP sensor placed on a human chest (**f**) comparable EKG readings from the bioresorbable device (left) compared to commercially available gel-based electrode readings (right) (**g**) a primary battery made of stacked cells of Mg and Mo tested in a PDMS dish containing PBS electrolyte solution. Reported output voltages of 1.5–1.6 V and discharge current density of 0.1 $mA{\cdot}cm^{-2}$ was sustained over 6 hours. (Reproduced with permission from Yin et al. [117]. Copyright 2014 John Wiley and Sons)

Table 2 General overview of main bioresorbable electronic devices and intended implications in healthcare

Purpose	Designs	Key devices	Implications
Energy supply	Battery	Primary and secondary batteries[a], photovoltaic cells[b]	Enable autonomous communication (i.e., RF antennas) and self-powered bioresorbable devices without the need of external energy sources
	Mechanical energy harvesting	Piezoelectric harvester, triboelectric nanogenerator[c]	
	Radiofrequency energy harvesting	Radiofrequency (RF) scavenger[d]	
	Graphene energy harvesting	Graphene flake, graphene oxide gelatin biocomposites[e]	
	Supercapacitance	Microsupercapacitor[f], organic supercapacitor[g]	
Biosensing	Electrophysiological and chemical sensing	EKG[h], ECoG and EEG[i], pH sensor[j], biochemical sensor[k], temperature sensor[l], deep tissue imaging[m], flow and motion sensor[n], hydration sensor[o]	Deliver direct and sensitive detection and imaging for diagnostics and acute disease, tissue, organ, and postoperative monitoring to guide patient-specific therapies
	Mechanical sensing	Pressure sensor, strain gauge[p]	
Therapeutics	Pharmacologic therapy	Heat-stimulated-controlled delivery device[q], multifunctional vascular stent with RRAM memory storage[r], optical waveguide[s]	Provide precise, controlled, and on-demand targeted therapy in situ
	Non-pharmacologic therapy	Electrical stimulus device for nerve regeneration and tissue stimulation[t], thermal therapy[u]	

[a][13, 25, 26, 34, 51, 52, 64, 108, 117]; [b][81]; [c][17, 18, 80, 120, 122]; [d][38, 72]; [e][70]; [f][73]; [g][68, 112]; [h][6, 42]; [i][58, 118]; [j][42, 58]; [k][3, 42, 84, 89]; [l][3, 58, 71]; [m][3]; [n][58, 97]; [o][89]; [p][6, 7, 17, 36, 58, 82]; [q][12, 71, 97, 104, 120]; [r][97]; [s][3]; [t][66, 122]; [u][36, 104]

3.1.1 Batteries

Transient primary and secondary batteries (i.e., non-rechargeable and rechargeable voltaic batteries, respectively) have been designed with and without demonstrated biocompatibility to date [38, 72]. Kelvin Fu and colleagues outlined five key criteria for successful design and performance of transient batteries including complete transience in the body; controllable desorption rates; mechanical properties and performance that meet device demands over specified timeframes; appropriate device dimensions; and compatibility with bioresorbable devices [13, 25, 34, 51, 52, 108, 117].

Yin and colleagues fulfilled these fundamental criteria with a fully resorbable, biocompatible primary battery (3 cm^3 × 1.3 cm^3 × 1.6 cm^3, ~3.5 g) composed of Mg foil anodes, Mo cathodes, and porous polyanhydride packaging that was permeable to hydrogen evolved from the battery [27]. Single cells of Mg/Fe, Mg/W, and Mg/Mo batteries had output voltages of about 0.75 V, 0.65 V, and 0.45 V, respec-

tively, in PBS electrolyte solution over 24 hours. To achieve comparable performance to conventional primary batteries, the bioresorbable batteries were assembled with four stacks of Mg-Mo cells to increase output voltage to 1.5–1.6 V and achieve a discharge current density of 0.1 $mA{\cdot}cm^{-2}$ sustained over 6 hours in PBS electrolyte solution (Fig. 3h) [117]. Potential pitting corrosion of metal foils or collective leakage of water through the porous polyanhydride overtime was used to explain the diminished stable lifetime of the stacked cells compared to the single cell batteries [35, 117].

Kim et al. developed a proof-of-concept edible sodium battery intended to directly supply power to self-sufficient, noninvasive devices for direct sensing of heart rate, core body temperature, chemicals, and metabolic activity. It was also envisaged to provide power for stimulation for gastrointestinal (GI) motility disorders and electrically mediated chemical release throughout the GI tract [117]. The battery was fabricated with flexible, rectangular electrodes (~2 mm × 0.4 mm) composed of silver nanowires dispersed through flexible poly(glycerol-co-sebacate)-cinnamate polymer, an activated carbon anode, and MgO_2 cathode. The battery was bent in half and placed into a gelatin capsule where current flow commenced once electrolyte solution reached the inside of the capsule [64]. Onset of activity can be adjusted by modifying encapsulating materials. In a 0.5 M isothermal solution of Na_2SO_4 at 37 °C, the battery supplied current to recording stainless steel electrodes to mimic an attached device up to 100 mA and then decreased gradually over the course of 5 hours. The energy density of the device could be improved by altering the cathode/anode mass ratios, increasing the amount of sodium content on the anode, and increasing the electrode mass density [64]. The battery is anticipated to be safe in vivo according to previously established biosafety and biocompatibility studies of each device component [64].

3.1.2 Mechanical Energy Harvesters

A bioresorbable mechanical energy harvester (MEH) using ZnO as the piezoelectric material was developed in 2013 by Dagdeviren et al. Piezoelectric energy harvesters produce energy by converting mechanical energy into electrical energy for low-power devices, such as microelectronics. The movement of the body can be used to power the energy supply [64]. Each mechanical energy harvester had a capacitor-type structure with a ZnO layer between bottom and top Mg electrodes (50 μm × 2 mm). There were six groups of ten capacitor ensembles connected in series by Mg interconnects creating a ~1 cm × 1 cm capacitor stage in the center of a silk fibroin substrate that was a few cm in length [18]. Conversion efficiency of the device was measured to be 0.28% under dry conditions but varies with mechanical load, physical dimensions, and elasticity of the substrate and piezoelectric components [18]. Lifetime of the energy harvester was not reported; however, a thin-film transistor with similar components without encapsulation reported in the same study exhibited steady function for over 3 hours and fully disappeared within 15 hours in DI water at room temperature [18].

The use of bioresorbable triboelectric generators for implantable devices has been reported by multiple authors. A voltage is produced in these generators by fluctuating the distance between two dissimilar materials capable of electron exchange. The arrangement includes an inner coating of metal electrodes followed by an insulating spacer in between the two metal coatings. Upon mechanical cycling, an electric potential is produced, which is capable of inducing an AC current between the metal electrodes [18]. In the study conducted by Zheng et al., a completely biodegradable and biocompatible triboelectric generator was developed using layers of commercially available polymers, like PLGA, PHB/V, PCL, and PVA, with a polymeric spacer in the center and Mg electrode layers. The nanogenerator (2 cm × 3 cm) was reported to have open-circuit voltage outputs ranging from 10 to 40 V with simulated biomechanical motion (1 Hz) depending on the polymer layers used. Further modification of output voltage could be executed by roughening the surfaces of the polymers through etching via immersion into sodium hydroxide (NaOH, 2 M) over a specified time frame (0–10 minutes). Output voltage increase with increasing etching time. Also, polymer selection dictates voltage output of the device, as each polymer possesses a different capacity of transferring or retaining electrons upon mechanical stimuli (i.e., triboelectric potential). In vivo studies using PLGA (75:25) and PVA encapsulating layers showed stable output for 14 days and less than 1 day, respectively. To demonstrate medical utility, the nanogenerator was linked to a rectifier and electrodes to apply an electric field to primary neurons to attempt cell alignment induction, which has been shown to be conducive to nerve repair. ImageJ results reported that 88% of cells exhibited alignment upon electrical stimulation (10 V/mm, 1 Hz) of 30 minutes per day for 5 days as opposed to disordered growth exhibited in the nerve cells with no electrical stimuli [12, 38, 80, 120, 122].

3.1.3 Microsupercapacitors

A flexible, bioresorbable microsupercapacitor, a type of electrochemical supercapacitor for storage and delivery of energy, was built onto a glass substrate using metal electrodes (W, Fe, or Mo) and a NaCl agarose hydrogel for the electrolyte with PLGA or polyanhydride encapsulating layers, respectively. The device was flexible and able to adhere to a finger nail demonstraing conformability to body tissues. Tungsten had the highest mechanical and equivalent series resistance (ESR) durability compared to Fe and Mo at 1000 cycles and 500 cycles, respectively. The device had stable capacitance for ~6 hours with PLGA packaging (10–15 μm) and extended up to 36 hours (10×10^{-3} M PBS, pH 7.4, 37 °C) with the addition of thicker, double-sided layers of a hydrophobic polyanhydride packaging material (150 μm) [73].

3.2 Biosensing

Standard clinical practice heavily relies on electronic implants for biosensing. Common applications being neurological diagnostics, traumatic brain injury monitoring, and care for cardiac events. Current conventional electronic sensors often lack flexibility, failing to conform to the curvilinear anatomy causing unnecessary mechanical stresses on surrounding tissues and necessitating device removal. Transient electronic biosensors can serve as a solution to existing mechanical restraints with no need for device removal [73]. Sensors outlined below have been designed for electrical sensing, pressure sensing, and biochemical sensing in applications ranging from wound healing, intracranial and organ pressure monitoring to pH, neurologic, and biomarker sensing. Furthermore, with advances in resorbable wireless communications and memory, computerized and stored data acquisition along with self-sufficient power supply is becoming possible to collect and store data from completely transient implantable devices for translation [14, 79, 118].

3.2.1 Electrophysiologic Monitoring

Lightweight, transient electrophysiological (EP) monitors have been developed from an organic electrochemical transistor (OECT) and multifunctional, elastic sensor using CMOS technology for uses in cardiovascular, muscle, and nerve monitoring. These transient systems are particularly advantageous over conventional electronics by minimizing e-waste, providing easy transport for short-term clinical needs, and avoiding sensor removal [35, 38, 41, 58, 89, 97]. The OECT device was composed of a solvent-cast PLGA substrate, gold source and drain, and PEDOT:PSS conductive components [11, 42]. Using this technology, an EKG capable of detecting 50 μV signals was fabricated with reported response times around 1.5 ms (0.1 M PBS at pH 7.4) with signal-to-noise ratios (S:N) comparable to standard Faradaic electrodes [11].

For high-resolution electrophysiological and postoperative monitoring Yu and colleagues developed three key bioresorbable devices for EKG recording, electrocorticography (ECoG) and electroencephalography (EEG) monitoring with operation times lasting between a few hours to 30 days for heart function tracking and spatiotemporal mapping of brain activity, respectively [11]. The neural electrode array was composed of a PLGA substrate layer, phosphorous-doped Si-NM electrodes and interconnects, and SiO_2 for insulation around interconnects and interlayer dielectrics [119]. Areas of highly doped Si served as terminal pads and external connections. In vivo comparison studies of the bioresorbable electrodes compared to control (commercial stainless steel microwave electrodes) embedded 0.5 mm from the cortical surface into the left hemisphere were completed up to 33 days with the bioresorbable device demonstrating a superior S:N compared to control after application of bicuculline methiodide to induce epileptic activity. A multiplexed neural electrode array was also fabricated for more efficient ECoG

sensing [119]. The flexible device consisted of PLGA as the substrate, mono-Si-NM as the semiconductor and neural interface electrodes, and SiO_2 as an insulating layer. SiO_2 and Si_3N_4 further served as gate dielectrics, interlayer dielectrics, and encapsulating layers with sensors and an external readout joined by electrical interconnects consisting of Mo [49, 119]. Based on the accelerated dissolution tests, the whole multiplexing device is expected to completely resorb in 6 months [119]. The microscale ECoG performance of a 64-electrode array was successfully used to visualize epileptic-related peaks after topical application of picrotoxin followed by immediate placement of the device onto the left hemisphere of the cortex in anaesthetized rats [119]. In future studies for epilepsy diagnostic applications, it would be ideal to increase operational lifetime as locating seizure origin takes 1–3 months of monitoring on average in practice. Somatosensory evoked potential (SSEP) studies were completed in vivo using the multiplexing device exhibiting the ability to record low-amplitude-induced cortical activity from mechanically stimulated whiskers. This device could also be used for monitoring of skeletal muscle tissue and organ function as well as early detection of implant failures (i.e., pressure and flow after coiling, vascular grafting, and repair of CSF leaks) during postoperative timeframes to evade expensive and invasive means of monitoring and consequences of neglecting implant failure [119].

3.2.2 Environmental Sensing

A multifunctional, completely bioresorbable wireless sensor was tested in vivo by Kang and colleagues for applications including but not limited to traumatic brain injury, extremity compartment syndromes, tissue stimulation, biomolecular sensing and recording. The device carried potential for temperature, intracranial pressure (ICP), fluid flow, motion, and/or pH sensing upon minor design modifications [118]. Furthermore, incorporation of chemical sensing, energy harvesting, and radiofrequency communication attachments is also possible [58]. The final device (1 mm × 2 mm × 0.08 mm) incorporated nanoporous silicon or Mg foil as the substrate with a cavity etched coated with a PLGA membrane to create an air pocket [58]. The piezoresistive component was a serpentine-shaped Si-NM placed on the perimeter of the etched gap where maximum strain was induced for a given applied pressure and the passivation layer was composed of SiO_2 [58]. Mo or Mg interconnect wires were used as the bridge between PLGA and the Mo wires for wireless communication with PLGA insulation [58]. A pressure range of 0–70 mmHg was detectable by this sensor with reliable operation up to 72 hours in deionized (DI) water (37 ˚C) and artificial cerebrospinal fluid (aCSF) using a 120 μm-thick polyanhydride encapsulation layer. A temperature sensor without an etched air pocket avoided water penetration for up to 6 days [58]. No evidence of device rejection was observed up to an 8-week time point in rats [58]. A PLLA-based piezoelectric device was also constructed for intra-organ pressure monitoring [58]. In this device, PLLA serves as the piezoelectric surrounded by Mo or Mg electrodes and is coated with a PLA encapsulation layer. The device undergoes complete dissolution after approximately 2 months [17].

An organic electrochemical sensor was developed to successfully sense dopamine and vitamin C by using electrodes made of PEDOT:PSS and silk fibroin as a substrate, which degraded within 4 weeks. Other sensors have been developed for bacterial sensing using conductive graphene components on a silk substrate to detect bacteria on tooth enamel [17]. Additionally, a novel, bioresorbable hydration sensor consisting of phosphorous-doped Si electrodes, Mg contacts and interconnects, SiO_2 dielectric, and PLGA substrate was used to monitor changes in skin moisture through impedance measurements comparably to a commercial moisture meter and was expected to completely disappear within a few months (0.1 M PBS at 37 °C). Hydration sensing could be used to monitor wound healing as both excess and inadequate hydration have negative implications for the wound healing process [35, 89].

3.2.3 Elastic Sensors for Electrophysical, Chemical, and Mechanical Sensing

Devices that need to accommodate high strains from body motion and curvature have been developed to create CMOS inverters, pH, pressure, and electrophysiological (EP) sensors. Stretchable sensors developed for monitoring tendon healing after surgery to guide patient-specific treatment regimens were created by designing a scalable, dual-functioning pressure sensor and strain gauge (12 mm × 7 mm × 1.4 mm) using the elastomer, POMaC, as encapsulating layers due to its softness comparable to body tissue and low tensile modulus to prevent interference with the healing process (Fig. 3e) [41]. The elastomer, PGS, was used as the dielectric material for the pressure sensor capacitor and nonadhesive layer in the strain gauge. Mg served as the electrodes supported by a PLLA substrate [7]. The device was capable of sensing strain 0–15% for five loading-unloading cycles and 0–100 kPa of pressure for six cycles with negligible hysteresis and S:N of 2:1. Moreover, the device was able to manage stable capacitance for over 20,000 cycles using applied relevant strain ranges for tendons (5–10%) along with 15–45 kPa of applied pressure with sustained function after 3.5 weeks in vivo [7]. No significant differences were found in immunochemistry analysis compared to silicone controls after 8 weeks. Other stretchable pressure sensors used PGS as a dielectric between Fe-Mg electrode layers taking a few months to completely degrade for cardiovascular monitoring [7].

Hwang and colleagues specially designed implantable devices capable of stretching up to ~30% while sustaining functionality. The design included Si nanoribbons with serpentine and noncoplanar interconnects joining device islands on the elastomeric substrate composed of POC. Under mechanical stress, the specially designed interconnects deform by in-plane and out-of-plane buckling while leaving device islands unaffected [42]. POC was chosen as a substrate due to its biocompatibility, controllable mechanical properties, biodegradability, and exceptional elasticity [6, 14]. The CMOS inverters consisted of Mg electrodes and interconnects, Si-NMs for the semiconducting nanoribbons, and SiO_2 for the gate and interlayer dielectrics and encapsulation layer. In each device, the interconnec-

tions were encapsulated with thin layers of POC to better perform under applied stress, prevent delamination, and for protection. SiO_2 and SiN_x dielectric materials were suggested to prolong device performance without substantial sacrifice to device sensitivity [42].

The hyperelastic device design was used to create a stretchable pH sensor and EP sensor [42]. In the pH sensor, Si nanoribbons underwent functionalization with 3-aminopropyltriethoxysilane. Under acidic conditions, the functionalized nanoribbons become protonated, changing surface charge, which serve as an electrostatic gate to subsequently diminish or gather charge carriers in doped n-type or p-type Si nanoribbons ($\sim 10^{20}$ cm^{-3}) permitting detection of pH changes. The pH sensors had a sensitivity of 0.1 ± 0.01 μS/pH for phosphorous-doped Si and 0.3 ± 0.02 μS/pH in boron-doped Si. The pH sensor containing p-type Si (200 nm) exhibited stable detection at 5 days (aqueous solution, pH 7.4, 37 °C) [42]. The EP sensors were attached topically to the chest and forearm of a patient to obtain EKG and electromyogram (EMG) readings (Fig. 3f) [42]. The serpentine meshes were composed of Mg and SiO_2 layers. Mg electrodes were coupled to the skin with a thin layer of POC between the two. Output EKG and EMG readings were compared to control (conventional gel electrode) (Fig. 3g), and devices were able to completely dissolve in pH 10 aqueous solution at room temperature.

3.3 Therapeutics

Developing bioresorbable electronic systems permits improved means of localized controlled release of drug delivery and on-demand non-pharmacologic (i.e., thermal and electric) therapies with envisioned indications not limited to nerve regeneration, bacterial infections, cancer therapy, and coronary artery disease [59, 66, 71, 97, 104]. Noteworthy advances in transient electronic therapeutic devices include heat-mediated drug delivery, noninvasive postsurgical electrical stimulation, and multifunctional capabilities sometimes incorporating memory storage and self-sufficient sources of power as summarized below.

3.3.1 Heat-Stimulated Drug Release

To manage postoperative infection secondary to *Staphylococcus aureus (S. aureus)* and *Escherichia coli (E. coli)*, Tao and colleagues designed a resorbable therapeutic device capable of remote-controlled, heat-stimulated drug release. The device consisted of a silk substrate, Mg containing resistor linked to a Mg heater with a MgO interlayer dielectric in between protected by a silk encapsulation layer [104]. The drug-loaded model of the device used an ampicillin-silk matrix that coated the encapsulation layer [104]. A remote primary coil placed within 1 mm of the receiving coil activated the device through near-field coupling. A steady, local temperature of 42 °C or 49 °C could be produced from the device for two 10-minute treatment intervals [104]. Increased temperatures caused simultaneous crystallization of the

silk fibroin and enhanced diffusion of ampicillin to augment its release into the surrounding milieu. Drug release could be controlled by tuning silk crystallinity and thickness of the encapsulation layer [104]. In vitro and in vivo experiments both demonstrated successful bacterial killing and visible surgical site healing with complete device dissolution within 15 days in vivo [104].

Multidrug release from an electrically active resorbable device was introduced by Lee and colleagues in 2015. Drug-containing lipids expanded to release three chemically dissimilar medications: parathyroid hormone (pTH), dextran, and doxorubicin, in response to remote-controlled heat stimuli [71]. The device components were comprised of Mo conductive pieces, and PLGA constituted the interconnects, dielectric layers and encapsulation with a novel multilayered lipid and cholesterol design to support embedded drugs with minute leakage over the course of months without heat stimuli. Inductively coupled coils caused temperature increases (41–45 °C) wirelessly by applying power from a waveform and radiofrequency generator to an external coil (1.0 W at 12.5–14 MHz). The regimen was able to be applied daily to release medication induced by temperature-related changes in lipid structure for up to 1 week [71]. Strategies employed to modify drug or drug dosages included substituting lipids to alter diffusivity of and attractive forces with loaded drugs, increasing the quantity of lipid layers, and tailoring lipid to drug ratios [71]. Moreover, biocompatibility was demonstrated with no significant increase in immune cells at the implantation site or weight loss in mice with implanted lipid containing devices compared to high-density polyethylene (HDPE) and the resorbable device without lipids, respectively [71].

3.3.2 Tissue Regeneration

Peripheral nerve injuries account for an astounding 3% of all trauma-related injuries. Peripheral nerve repair procedures account for 5,000,000 disability days in the USA, and only half of patients victim to peripheral nerve damage report satisfactory functional recovery after surgical intervention [87, 92]. Studies have demonstrated improved functional recovery while reducing recovery times with electrical stimulation at the surgical site. An implantable, bioresorbable, and self-operating electrical stimulating device was reported to provide direct electrical stimulation postoperatively in 1 hour doses for up to 6 days with superior effects to a negative control (no stimulation) in rats, and required no surgical removeal unlike its predecessors [32, 66]. The transient device (40 mm × 10 mm × 200 μm) combined a radiofrequency power harvester using a loop antenna composed of Mg, a dielectric interlayer of PLGA, a doped Si-NM radiofrequency diode with Mg electrodes, and a parallel plate capacitor made of a SiO_2 dielectric layer in between the conducting layers linked to an electrical interface formed from protruding electrodes of the energy harvester embedded in PLGA. Strips of Mg or Mo for electrical connections were wrapped around the nerve [66]. The electrical stimulus is delivered from the receiving antenna to the electrical connections to the nerves (Fig. 3a). Longer post-surgical stimulation regimens showed to be superior in increasing denervated muscle mass, reaction times, and force measurements (1 vs. 6 days of stimulation) [66].

With a few refinements, other treatments can be explored using this technology including muscle, organ, spinal cord, and cardiac tissue stimulation therapies [66].

3.3.3 Multifunctional Therapies

Multifunctional sensing and treatment devices have been a substantial advancement in bioresorbable electronics to provide highly sensitive and minimally invasive monitoring and targeted treatment options for patients, and in some instances, overcoming the drawback of external energy supplies necessary for previously developed resorbable electronics [97, 120].

Son and colleagues engineered a flexible, bioresorbable vascular stent (210 μm thickness, 5.5 mm diameter, ~10 mm length) capable of controllable drug release, scavenging of reactive oxygen species (ROS), flow and temperature sensing, resistive random-access memory (RRAM) data storage, and wireless data communication [97]. Components of this device included Mg, MgO, Mg alloys, Zn, ZnO, gold (Au), SiO_2, cerium dioxide (CeO_2), and PLA [97]. Cerium dioxide nanoparticles scavenged reactive oxygen species, while near-infrared (IR) responsive (800 nm) Au-nanorod (NR) core nanoparticles with mesoporous silica shells released rapamycin for restenosis prophylaxis. A temperature sensor associated with thermal regulation acted to reduce the risk of heat-induced necrosis and embolization. Conductance of Mg in PBS with PLA (120 mm) and MgO (300 nm) insulation was reported to be stable for up to 66 days, whereas without the PLA layer, the Mg containing electronic components degraded within 30 minutes.

By using a triboelectric generator, an autonomous sensing and responsive therapeutic device was developed by Zhang and colleagues with proof-of-concept in vivo demonstration of applicability in epilepsy and anti-infective treatments [120]. Up to 60 V of open-circuit voltage was able to be generated upon 2 Hz stimuli from a device composed of silk and Mg [120]. Stable operation of the triboelectric nanogenerators was demonstrated to vary from 10 minutes to 10 hours by tuning surface features and encapsulating layers [120]. For epilepsy management, the device monitored and detected epileptic signals (Fig. 3b) to induce thermally mediated drug release of phenobarbital from silk films (Fig. 3c) while concomitantly delivering electronic communication for seizure identification and alert notification to a mobile device (Fig. 3d) [120].

4 Summary and Outlook

Since the development of transient electronics in the early 2000s, great strides have been achieved in advanced applications of biodegradable electronic devices in an attempt to address unsatisfactory clinical sensing and treatment in acute scenarios. Current bioresorbable electronics are primarily constituted of thin layers of conducting, semiconducting, and insulating materials capable of degrading in the body

over finite timeframes. Engineering designs have successfully incorporated active (i.e., transistors, diodes) and passive (i.e., resistors, inductors, capacitors) components to develop bioresorbable medical devices like pressure and temperature sensors for intracranial pressure monitoring, direct, self-powered electrically stimulating scaffolds for nerve regeneration, electrocardiograms and multifunctional stents for cardiovascular management, and remote-controlled drug release devices for targeted drug delivery. Benefits to using bioresorbable electronic implants include evasion of secondary surgeries for device removal, sensitive and direct tissue interfacing, and reduced risk of tissue damage due to device migration, infection, or long-term immune-mediated reactions. Furthermore, bioresorbable electronics degrade completely into biocompatible by-products reducing the amount of environmental and economic strains attributed to electronic waste and associated recycling costs.

Aside from the advances made and the promising outlook of transient electronic devices for improved patient care, there still remains inadequacies before implemenation into a clinical setting is feasible. Namely, lack of tightly controlled dissolution and device lifetimes, limited manufacturing sites for scalability, few multifunctional designs, and high-power, self-sufficient energy supplies inhibit implementation into present healthcare practice. Areas of research dedicated to encapsulation materials and novel transient device designs, materials processing, and wireless communication are critical to attaining desired device performances with practical translatability. Unexplored and combinations of existing device designs and materials can bring transient electronics closer toward reducing unnecessary adverse effects and waste in the clinical setting while considerably enhancing biosensing and patient-specific treatments not achievable by current non-resorbable electronic technologies.

References

1. Acar, H., et al. (2014). Study of physically transient insulating materials as a potential platform for transient electronics and bioelectronics. *Advanced Functional Materials, 24*(26), 4135–4143. https://doi.org/10.1002/adfm.201304186.
2. Adnan, S. M., et al. (2016). Water-soluble glass substrate as a platform for biodegradable solid-state devices. *IEEE Journal of the Electron Devices Society, 4*(6), 490–494. https://doi.org/10.1109/JEDS.2016.2606340.
3. Bai, W., et al. (2018). Flexible transient optical waveguides and surface-wave biosensors constructed from monocrystalline silicon. *Advanced Materials, 30*(32), 1–12. https://doi.org/10.1002/adma.201801584.
4. Balde, C. P., et al. (2017). The global e-waste monitor 2017. *United Nations University, IAS – SCYCLE, Bonn, Germany., 35*, 3397. https://doi.org/10.1016/j.proci.2014.05.148.
5. Bettinger, C. J., & Bao, Z. (2010). Organic thin-film transistors fabricated on resorbable biomaterial substrates. *Advanced Materials, 22*(5), 651–655. https://doi.org/10.1002/adma.200902322.
6. Boutry, C. M., et al. (2015). A sensitive and biodegradable pressure sensor array for cardiovascular monitoring. *Advanced Materials, 27*(43), 6954–6961. https://doi.org/10.1002/adma.201502535.

7. Boutry, C. M., et al. (2018). A stretchable and biodegradable strain and pressure sensor for orthopaedic application. *Nature Electronics*. Springer US, *1*(5), 314–321. https://doi.org/10.1038/s41928-018-0071-7.
8. Bowen, P. K., Drelich, J., & Goldman, J. (2013). Zinc exhibits ideal physiological corrosion behavior for bioabsorbable stents. *Advanced Materials, 25*(18), 2577–2582. https://doi.org/10.1002/adma.201300226.
9. Brenckle, M. A., et al. (2015). Modulated degradation of transient electronic devices through multilayer silk fibroin pockets. *ACS Applied Materials and Interfaces, 7*(36), 19870–19875. https://doi.org/10.1021/acsami.5b06059.
10. Callister Jr, W. D. (University of U.) and Rethwisch, D. G. (University of I). (2014). *Materials Science and Engineering: An Introduction*. 9th edn. Edited by D. Sayre, J. Metzger, and M. Price. Hoboken: Wiley.
11. Campana, A., et al. (2014). Electrocardiographic recording with conformable organic electrochemical transistor fabricated on resorbable bioscaffold. *Advanced Materials, 26*(23), 3874–3878. https://doi.org/10.1002/adma.201400263.
12. Chen, Y., et al. (2015). A touch-communication framework for drug delivery based on a transient microbot system. *IEEE Transactions on Nanobioscience, 14*(4), 397–408. https://doi.org/10.1109/TNB.2015.2395539.
13. Chen, Y., et al. (2016). Physical–chemical hybrid transiency: A fully transient li-ion battery based on insoluble active materials. *Journal of Polymer Science, Part B: Polymer Physics, 54*(20), 2021–2027. https://doi.org/10.1002/polb.24113.
14. Chen, Y., et al. (2018). Advances in materials for recent low-profile implantable bioelectronics. *Materials, 11*(4), 1–24. https://doi.org/10.3390/ma11040522.
15. Cheng, H. (2016). Inorganic dissolvable electronics: Materials and devices for biomedicine and environment. *Journal of Materials Research, 31*(17), 2549–2570. https://doi.org/10.1557/jmr.2016.289.
16. Cheng, H., & Vepachedu, V. (2016). Recent development of transient electronics. *Theoretical and Applied Mechanics Letters*. Elsevier Ltd, *6*(1), 21–31. https://doi.org/10.1016/j.taml.2015.11.012.
17. Curry, E. J., et al. (2018). Biodegradable piezoelectric force sensor. *Proceedings of the National Academy of Sciences, 115*(5), 909–914. https://doi.org/10.1073/pnas.1710874115.
18. Dagdeviren, C., et al. (2013). Transient, biocompatible electronics and energy harvesters based on ZnO. *Small, 9*(20), 3398–3404. https://doi.org/10.1002/smll.201300146.
19. Dey, J., et al. (2008). Development of biodegradable crosslinked urethane-doped polyester elastomers. *Biomaterials*. Elsevier Ltd, *29*(35), 4637–4649. https://doi.org/10.1016/j.biomaterials.2008.08.020.
20. Erdogan, S., Kaya, M., & Akata, I. (2017). Chitin extraction and chitosan production from cell wall of two mushroom species (Lactarius vellereus and Phyllophora ribis), *AIP Conference Proceedings*, 1809. https://doi.org/10.1063/1.4975427.
21. Fedoročková, A., & Raschman, P. (2008). Effects of pH and acid anions on the dissolution kinetics of MgO. *Chemical Engineering Journal, 143*(1–3), 265–272. https://doi.org/10.1016/j.cej.2008.04.029.
22. Feig, V. R., Tran, H., & Bao, Z. (2018). Biodegradable polymeric materials in degradable electronic devices. *ACS Central Science, 4*(3), 337–348. https://doi.org/10.1021/acscentsci.7b00595.
23. Forrest, S. R. (2004). The path to ubiquitous and low-cost organic electronic appliances on plastic. *Nature, 428*(6986), 911–918. https://doi.org/10.1038/nature02498.
24. Fraietta, J. A., & Kietrys, D. M. (2015). Factors affecting the immune system. In K. Helgeson & B. Shelly (Eds.), *Pathology: implications for the physical therapist* (4th ed., pp. 276–279). Saunders/Elsevier: St. Louis. Available at: https://books.google.com/books?id=1he0BQAAQBAJ&pg=PA277&lpg=PA277&dq=ZINC+has+been+identified+as+a+cofactor+for+over+70 +different+enzymes&source=bl&ots=fYFUyYEp6Q&sig=5MF32GPY50jyv4B8x5IYcgzn9fE&hl=en&sa=X&ved=2ahUKEwj0wcTqpuHdAhWLuFMKHTKuA78Q6AEwBHoECAUQ.

25. Fu, K., et al. (2015). Transient rechargeable batteries triggered by Cascade reactions. *Nano Letters, 15*(7), 4664–4671. https://doi.org/10.1021/acs.nanolett.5b01451.
26. Fu, K., et al. (2016). All-component transient lithium-ion batteries. *Advanced Energy Materials, 6*(10), 1–9. https://doi.org/10.1002/aenm.201502496.
27. Fu, K. K., et al. (2016). Transient electronics: Materials and devices. *Chemistry of Materials, 28*(11), 3527–3539. https://doi.org/10.1021/acs.chemmater.5b04931.
28. Gao, Y., Zhang, Y., et al. (2017). Moisture-triggered physically transient electronics. *Science Advances, 3*(9), 1–9. https://doi.org/10.1126/sciadv.1701222.
29. Gao, Y., Sim, K., et al. (2017). Thermally triggered mechanically destructive electronics based on electrospun poly(ϵ-caprolactone) nanofibrous polymer films. *Scientific Reports*. Springer US, *7*(1), 1–8. https://doi.org/10.1038/s41598-017-01026-6.
30. Gentile, P., et al. (2014). An overview of poly(lactic-co-glycolic) acid (PLGA)-based biomaterials for bone tissue engineering. *International Journal of Molecular Sciences, 15*, 3640–3659. https://doi.org/10.3390/ijms15033640.
31. Göpferich, A., & Tessmar, J. (2002). Polyanhydride degradation and erosion. *Advanced Drug Delivery Reviews, 54*(7), 911–931. https://doi.org/10.1016/S0169-409X(02)00051-0.
32. Gordon, T. (2016). Electrical stimulation to enhance axon regeneration after peripheral nerve injuries in animal models and humans. *Neurotherapeutics, 13*(2), 295–310. https://doi.org/10.1007/s13311-015-0415-1.
33. He, X., et al. (2016). Transient resistive switching devices made from egg albumen dielectrics and dissolvable electrodes. *ACS Applied Materials and Interfaces, 8*(17), 10954–10960. https://doi.org/10.1021/acsami.5b10414.
34. Huang, X., et al. (2018). A fully biodegradable battery for self-powered transient implants. *Small, 14*(28), 1–8. https://doi.org/10.1002/smll.201800994.
35. Huang, X. (2018). Materials and applications of bioresorbable electronics. *Journal of Semiconductors, 39*(1), 011003. https://doi.org/10.1088/1674-4926/39/1/011003.
36. Hwang, S.-W., et al. (2012). A physically transient form of silicon electronics. *Science, 337*(6102), 1640–1644. https://doi.org/10.1126/science.1142996.
37. Hwang, S. W., Kim, D. H., et al. (2013). Materials and fabrication processes for transient and bioresorbable high-performance electronics. *Advanced Functional Materials, 23*(33), 4087–4093. https://doi.org/10.1002/adfm.201300127.
38. Hwang, S. W., Huang, X., et al. (2013). Materials for bioresorbable radio frequency electronics. *Advanced Materials, 25*(26), 3526–3531. https://doi.org/10.1002/adma.201300920.
39. Hwang, S. W., Park, G., Cheng, H., et al. (2014). 25th anniversary article: Materials for high-performance biodegradable semiconductor devices. *Advanced Materials, 26*(13), 1992–2000. https://doi.org/10.1002/adma.201304821.
40. Hwang, S. W., Park, G., Edwards, C., et al. (2014). Dissolution chemistry and biocompatibility of single-crystalline silicon nanomembranes and associated materials for transient electronics. *ACS Nano, 8*(6), 5843–5851. https://doi.org/10.1021/nn500847g.
41. Hwang, S. W., Song, J. K., et al. (2014). High-performance biodegradable/transient electronics on biodegradable polymers. *Advanced Materials, 26*(23), 3905–3911. https://doi.org/10.1002/adma.201306050.
42. Hwang, S. W., et al. (2015). Biodegradable elastomers and silicon nanomembranes/nanoribbons for stretchable, transient electronics, and biosensors. *Nano Letters, 15*(5), 2801–2808. https://doi.org/10.1021/nl503997m.
43. Institute of Medicine (US) Panel on Micronutrients. (2001). *Iron*. Washington D.C.: National Academies Press (US).
44. Institute of Medicine (US) Panel on Micronutrients. (2001). Molybdenum. In *Dietary reference intakes for Vitamin A, Vitamin K, Arsenic, Boron, Chromium, Copper, Iodine, Iron, Manganese, Molybdenum, Nickel, Silicon, Vanadium, and Zinc* (p. 420). Washington, D.C.: National Academies Press (US).
45. Institute of Medicine (US) Panel on Micronutrients. (2001). Zinc. In *Dietary reference intakes for Vitamin A, Vitamin K, Arsenic, Boron, Chromium, Copper, Iodine, Iron,*

Manganese, Molybdenum, Nickel, Silicon, Vanadium, and Zinc (pp. 442–444). Washington, D.C.: National Academies Press (US).
46. Irimia-Vladu, M., et al. (2010). Biocompatible and biodegradable materials for organic field-effect transistors. *Advanced Functional Materials, 20*(23), 4069–4076. https://doi.org/10.1002/adfm.201001031.
47. Irimia-Vladu, M., Głowacki, E. D., et al. (2012). Green and biodegradable electronics. *Materials Today*. Elsevier Ltd, *15*(7–8), 340–346. https://doi.org/10.1016/S1369-7021(12)70139-6.
48. Irimia-Vladu, M., Głowacki, E. D., et al. (2012). Indigo – a natural pigment for high performance ambipolar organic field effect transistors and circuits. *Advanced Materials, 24*(3), 375–380. https://doi.org/10.1002/adma.201102619.
49. Irwin, J. D., & Kerns Jr., D. V. (1995). In A. Apt (Ed.), *Introduction to electrical engineering*. Upper Saddle River: Prentice-Hall.
50. Janotti, A., & Walle, C. G. Van De (2009). Fundamentals of zinc oxide as a semiconductor. *72*(12). https://doi.org/10.1088/0034-4885/72/12/126501.
51. Jia, X., et al. (2016). Toward biodegradable Mg-air bioelectric batteries composed of silk fibroin-polypyrrole film. *Advanced Functional Materials, 26*(9), 1454–1462. https://doi.org/10.1002/adfm.201503498.
52. Jia, X., et al. (2017). A biodegradable thin-film magnesium primary battery using silk fibroin−ionic liquid polymer electrolyte. *ACS Energy Letters, 2*(4), 831–836. https://doi.org/10.1021/acsenergylett.7b00012.
53. Jiang, H. L., & Zhu, K. J. (1999). Preparation, characterization and degradation characteristics of polyanhydrides containing poly(ethylene glycol). *Polymer International*, *48*(1), 47–52. https://doi.org/10.1002/(SICI)1097-0126(199901)48:1<47::AID-PI107>3.0.CO;2-X.
54. Jin, S. H., et al. (2014). Solution-processed single-walled carbon nanotube field effect transistors and bootstrapped inverters for disintegratable, transient electronics. *Applied Physics Letters, 105*(1), 013506. https://doi.org/10.1063/1.4885761.
55. Kang, S. K., et al. (2014). Dissolution behaviors and applications of silicon oxides and nitrides in transient electronics. *Advanced Functional Materials, 24*(28), 4427–4434. https://doi.org/10.1002/adfm.201304293.
56. Kang, S. K., Hwang, S. W., et al. (2015). Biodegradable thin metal foils and spin-on glass materials for transient electronics. *Advanced Functional Materials, 25*(12), 1789–1797. https://doi.org/10.1002/adfm.201403469.
57. Kang, S. K., Park, G., et al. (2015). Dissolution chemistry and biocompatibility of silicon- and germanium-based semiconductors for transient electronics. *ACS Applied Materials and Interfaces, 7*(17), 9297–9305. https://doi.org/10.1021/acsami.5b02526.
58. Kang, S. K., et al. (2016). Bioresorbable silicon electronic sensors for the brain. *Nature*. Nature Publishing Group, *530*(7588), 71–76. https://doi.org/10.1038/nature16492.
59. Kang, S. K., et al. (2018). Advanced materials and devices for bioresorbable electronics. *Accounts of Chemical Research*. American Chemical Society, *51*(5), 988–998. https://doi.org/10.1021/acs.accounts.7b00548.
60. Karandikar, S., et al. (2017). Nanovaccines for oral delivery-formulation strategies and challenges. *Nanostructures for Oral Medicine*. Elsevier Inc. https://doi.org/10.1016/B978-0-323-47720-8.00011-0.
61. Kim, D., et al. (2008). Materials and noncoplanar mesh designs for integrated circuits with linear elastic responses to extreme mechanical deformations. *Proceedings of the National Academy of Sciences, 105*(48), 1–6.
62. Kim, D. H., et al. (2009). Silicon electronics on silk as a path to bioresorbable, implantable devices. *Applied Physics Letters, 95*(13), 93–96. https://doi.org/10.1063/1.3238552.
63. Kim, D. H., et al. (2010). Dissolvable films of silk fibroin for ultrathin conformal bio-integrated electronics. *Nature Materials, 9*(6), 1–7. https://doi.org/10.1038/nmat2745.
64. Kim, Y. J., et al. (2013). Self-deployable current sources fabricated from edible materials. *Journal of Materials Chemistry B, 1*(31), 3781–3788. https://doi.org/10.1039/c3tb20183j.

65. Ko, J., et al. (2017). Human hair keratin for biocompatible flexible and transient electronic devices. *ACS Applied Materials and Interfaces, 9*(49), 43004–43012. https://doi.org/10.1021/acsami.7b16330.
66. Koo, J., et al. (2018). Wireless bioresorbable electronic system enables sustained nonpharmacological neuroregenerative therapy. *Nature Medicine*. Springer US*, 24*, 1830–1836. https://doi.org/10.1038/s41591-018-0196-2.
67. Kumar, A., Holuszko, M., & Espinosa, D. C. R. (2017). E-waste: An overview on generation, collection, legislation and recycling practices. *Resources, Conservation and Recycling*. Elsevier B.V.*, 122*, 32–42. https://doi.org/10.1016/j.resconrec.2017.01.018.
68. Kumar, P., et al. (2016). Melanin-based flexible supercapacitors. *Journal of Materials Chemistry C*. Royal Society of Chemistry*, 4*(40), 9516–9525. https://doi.org/10.1039/c6tc03739a.
69. Labet, M., & Thielemans, W. (2009). Synthesis of polycaprolactone: A review. *Chemical Society Reviews, 38*(12), 3484–3504. https://doi.org/10.1039/b820162p.
70. Landi, G., et al. (2017). Differences between graphene and graphene oxide in gelatin based systems for transient biodegradable energy storage applications. *Nanotechnology*. IOP Publishing*, 28*(5), 054005. https://doi.org/10.1088/1361-6528/28/5/054005.
71. Lee, C. H., Kim, H., et al. (2015). Biological lipid membranes for on-demand, wireless drug delivery from thin, bioresorbable electronic implants. *NPG Asia Materials*. Nature Publishing Group*, 7*(11), e227–e229. https://doi.org/10.1038/am.2015.114.
72. Lee, C. H., Jeong, J. W., et al. (2015). Materials and wireless microfluidic systems for electronics capable of chemical dissolution on demand. *Advanced Functional Materials, 25*(9), 1338–1343. https://doi.org/10.1002/adfm.201403573.
73. Lee, G., et al. (2017). Fully biodegradable microsupercapacitor for power storage in transient electronics. *Advanced Energy Materials, 7*(18), 1–12. https://doi.org/10.1002/aenm.201700157.
74. Lee, Y. K., Yu, K. J., Song, E., Farimani, A. B., et al. (2017). Dissolution of monocrystalline silicon nanomembranes and their use as encapsulation layers and electrical interfaces in water-soluble electronics. https://doi.org/10.1021/acsnano.7b06697.
75. Lee, Y. K., Yu, K. J., Song, E., Barati Farimani, A., et al. (2017). Dissolution of monocrystalline silicon nanomembranes and their use as encapsulation layers and electrical interfaces in water-soluble electronics. *ACS Nano, 11*(12), 12562–12572. https://doi.org/10.1021/acsnano.7b06697.
76. Lei, T., et al. (2017). Biocompatible and totally disintegrable semiconducting polymer for ultrathin and ultralightweight transient electronics. *Proceedings of the National Academy of Sciences, 114*(20), 5107–5112. https://doi.org/10.1073/pnas.1701478114.
77. Li, R., et al. (2013). An analytical model of reactive diffusion for transient electronics. *Advanced Functional Materials, 23*(24), 3106–3114. https://doi.org/10.1002/adfm.201203088.
78. Li, R., et al. (2017). Recent progress on biodegradable materials and transient electronics. *Bioactive Materials*. Elsevier Ltd*, 3*(3), 322–333. https://doi.org/10.1016/j.bioactmat.2017.12.001.
79. Li, R., Wang, L., & Yin, L. (2018). Materials and devices for biodegradable and soft biomedical electronics. *Materials, 11*(2108), 1–23. https://doi.org/10.3390/ma11112108.
80. Liang, Q., et al. (2017). Recyclable and green triboelectric nanogenerator. *Advanced Materials, 29*(5). https://doi.org/10.1002/adma.201604961.
81. Lu, L., et al. (2018). Biodegradable monocrystalline silicon photovoltaic microcells as power supplies for transient biomedical implants. *Advanced Energy Materials, 8*(16), 1–8. https://doi.org/10.1002/aenm.201703035.
82. Luo, M., et al. (2014). A microfabricated wireless RF pressure sensor made completely of biodegradable materials. *Journal of Microelectromechanical Systems, 23*(1), 4–13. https://doi.org/10.1109/JMEMS.2013.2290111.
83. Makadia, H. K., & Siegel, S. J. (2011). Poly Lactic-co-Glycolic Acid (PLGA) as biodegradable controlled drug delivery carrier. *Polymers, 3*(763), 1377–1397. https://doi.org/10.3390/polym3031377.

84. Mannoor, M. S., et al. (2012). Graphene-based wireless bacteria detection on tooth enamel. *Nature Communications*. Nature Publishing Group, *3*, 763–768. https://doi.org/10.1038/ncomms1767.
85. Markoulaki, S., et al. (2009). Development of aliphatic biodegradable photoluminescent polymers. *Proceedings of the National Academy of Sciences, 106*(28), 11818–11819. https://doi.org/10.1073/pnas.0906359106.
86. Meitl, M. A., et al. (2006). Transfer printing by kinetic control of adhesion to an elastomeric stamp. *Nature Materials, 5*(1), 33–38. https://doi.org/10.1038/nmat1532.
87. Mobini, S., et al. (2017). Recent advances in strategies for peripheral nerve tissue engineering. *Current Opinion in Biomedical Engineering, 4*, 134–142. https://doi.org/10.1016/j.cobme.2017.10.010.
88. Najafabadi, A. H., et al. (2014). Biodegradable nanofibrous polymeric substrates for generating elastic and flexible electronics. *Advanced Materials, 26*(33), 5823–5830. https://doi.org/10.1002/adma.201401537.
89. Pal, R. K., et al. (2016). Conducting polymer-silk biocomposites for flexible and biodegradable electrochemical sensors. *Biosensors and Bioelectronics*. Elsevier, *81*, 294–302. https://doi.org/10.1016/j.bios.2016.03.010.
90. Park, S., et al. (2013). Inorganic/organic multilayer passivation incorporating alternating stacks of organic/inorganic multilayers for long-term air-stable organic light-emitting diodes. *Organic Electronics: physics, materials, applications*. Elsevier B.V., *14*(12), 3385–3391. https://doi.org/10.1016/j.orgel.2013.09.045.
91. Patrick, E., et al. (2011). Corrosion of tungsten microelectrodes used in neural recording applications. *Journal of Neuroscience Methods*. Elsevier B.V., *198*(2), 158–171. https://doi.org/10.1016/j.jneumeth.2011.03.012.
92. Pfister, B. J., et al. (2011). Biomedical engineering strategies for peripheral nerve repair: surgical applications, state of the art, and future challenges. *Critical Reviews in Biomedical Engineering, 39*(2), 81–124. doi: 2809b9b432c80c2c,0fb500fc3eef5342 [pii].
93. Pomerantseva, I., et al. (2009). Degradation behavior of poly(glycerol sebacate). *Journal of Biomedical Materials Research Part A*, *91*(4), 1038–1047. https://doi.org/10.1002/jbm.a.32327.
94. Rahman, H. U., et al. (2013). Fabrication and characterization of PECVD silicon nitride for RF MEMS applications. *Microsystem Technologies, 19*(1), 131–136. https://doi.org/10.1007/s00542-012-1522-0.
95. Sabir, M. I., Xu, X., & Li, L. (2009). A review on biodegradable polymeric materials for bone tissue engineering applications. *Journal of Materials Science, 44*(21), 5713–5724. https://doi.org/10.1007/s10853-009-3770-7.
96. Shan, D., et al. (2018). Development of citrate-based dual-imaging enabled biodegradable electroactive polymers. *Advanced Functional Materials, 28*(34), 1801787. https://doi.org/10.1002/adfm.201801787.
97. Son, D., et al. (2015). Bioresorbable electronic stent integrated with therapeutic nanoparticles for endovascular diseases. *ACS Nano, 9*(6), 5937–5946. https://doi.org/10.1021/acsnano.5b00651.
98. Song, G., & Song, S. (2007). A possible biodegradable magnesium implant material. *Advanced Engineering Materials, 9*(4), 298–302. https://doi.org/10.1002/adem.200600252.
99. Stolica, N. (1985). Molybdenum. In A. J. Bard, R. Parsons, & J. Jordan (Eds.), *Standard potentials in aqueous solution* (pp. 462–483). New York: Marcel Dekker, Inc. Available at: https://books.google.com/books?id=XoZHDwAAQBAJ.
100. Su, L., et al. (2014). Study on the antimicrobial properties of citrate-based biodegradable study on the antimicrobial properties of citrate-based biodegradable polymers. *Frontiers in Bioengineering and Biotechnology, 2*(23). https://doi.org/10.3389/fbioe.2014.00023.
101. Sun, S., et al. (2016). The role of pretreatment in improving the enzymatic hydrolysis of lignocellulosic materials. *Bioresource Technology*. Elsevier Ltd, *199*, 49–58. https://doi.org/10.1016/j.biortech.2015.08.061.

102. Sun, Y., & Rogers, J. A. (2007). Inorganic semiconductors for flexible electronics. *Advanced Materials, 19*(15), 1897–1916. https://doi.org/10.1002/adma.200602223.
103. Tanskanen, P. (2013). Management and recycling of electronic waste. *Acta Materialia*. Acta Materialia Inc., *61*(3), 1001–1011. https://doi.org/10.1016/j.actamat.2012.11.005.
104. Tao, H., et al. (2014). Silk-based resorbable electronic devices for remotely controlled therapy and in vivo infection abatement. *Proceedings of the National Academy of Sciences, 111*(49), 17385–17389. https://doi.org/10.1073/pnas.1407743111.
105. Tao, H., Kaplan, D. L., & Omenetto, F. G. (2012). Silk materials - a road to sustainable high technology. *Advanced Materials, 24*(21), 2824–2837. https://doi.org/10.1002/adma.201104477.
106. Thimbleby, H. (2013). Technology and the future of healthcare. *Journal of Public Health Research, 2*(28), 160–167. https://doi.org/10.4081/arc.2013.e14.
107. Trolier-McKinstry, S. (Pennsylvania S. U.) and Newnham, R. (Pennsylvania S. U.) (2018) *Materials engineering: Bonding, structure, and structure-property relationships*. 1st edn. New York: Cambridge University Press.
108. Tsang, M., et al. (2015). Biodegradable magnesium/iron batteries with polycaprolactone encapsulation: A microfabricated power source for transient implantable devices. *Microsystems & Nanoengineering*. Taylor & Francis, 15024. https://doi.org/10.1038/micronano.2015.24.
109. Turner, R. E. (2006). Nutrition during pregnancy. In M. E. Shils et al. (Eds.), *Modern nutrition in health and disease* (10th ed., p. 778). Philadelphia: Lippincott Williams & Wilkins. Available at: https://books.google.com/books?id=S5oCjZZZ1ggC&printsec=frontcover&vq=molybdenum&source=gbs_ge_summary_r&cad=0#v=onepage&q=molybdenum&f=false.
110. Uwitonze, A. M., & Razzaque, M. S. (2018). Role of magnesium in vitamin D activation and function. *The Journal of the American Osteopathic Association, 118*(3), 181. https://doi.org/10.7556/jaoa.2018.037.
111. Vanýsek, P. (2012). Electrochemical series. *Handbook of Chemistry and Physics, 93*, 5–80.
112. Wang, X., et al. (2016). Food-materials-based edible supercapacitors. *Advanced Materials Technologies, 1*(3), 1600059. https://doi.org/10.1002/admt.201600059.
113. Wang, Y., et al. (2002). A tough biodegradable elastomer. *Nature Biotechnology, 20*(6), 602–606. https://doi.org/10.1038/nbt0602-602.
114. Witte, F., & Eliezer, A. (2012). Biodegradable metals. In N. Eliaz (Eds.), Degradation of Implant Materials (pp. 93-109). New York: Springer. Available at: https://www.google.com/books/edition/Degradation_of_Implant_Materials/NGydrqQb_CcC?hl=en&gbpv=0.
115. Yang, J., Webb, A. R., & Ameer, G. A. (2004). Novel citric acid-based biodegradable elastomers for tissue engineering. *Advanced Materials, 16*(6), 511–516. https://doi.org/10.1002/adma.200306264.
116. Yin, L., Cheng, H., et al. (2014). Dissolvable metals for transient electronics. *Advanced Functional Materials, 24*(5), 645–658. https://doi.org/10.1002/adfm.201301847.
117. Yin, L., Huang, X., et al. (2014). Materials, designs, and operational characteristics for fully biodegradable primary batteries. *Advanced Materials, 26*(23), 3879–3884. https://doi.org/10.1002/adma.201306304.
118. Yu, K. J., et al. (2016). Bioresorbable silicon electronics for transient spatiotemporal mapping of electrical activity from the cerebral cortex. *Nature Materials, 15*(7), 782–791. https://doi.org/10.1038/nmat4624.
119. Yu, X., et al. (2018). Materials, processes, and facile manufacturing for Bioresorbable electronics: A review. *Advanced Materials, 30*(28), 1–27. https://doi.org/10.1002/adma.201707624.
120. Zhang, Y., et al. (2018). Self-powered multifunctional transient bioelectronics. *Small, 14*(35), 1802050. https://doi.org/10.1002/smll.201802050.
121. Zhang, Z., Tsang, M., & Chen, I. W. (2016). Biodegradable resistive switching memory based on magnesium difluoride. *Nanoscale*. Royal Society of Chemistry, *8*(32), 15048–15055. https://doi.org/10.1039/c6nr03913h.

122. Zheng, Q., et al. (2016). Biodegradable triboelectric nanogenerator as a life-time designed implantable power source. *Science Advances, 2*(3), 1–9. https://doi.org/10.1126/sciadv.1501478.
123. Duncanson, A., & Stevenson, R. W. H. (1958). Some properties of magnesium fluoride crystallized from the melt. *Proceedings of the Physical Society, 72*(6), 1001–1006.
124. Horan, R. L., et al. (2005). In vitro degradation of silk fibroin. *Biomaterials, 26*(17), 3385–3393. https://doi.org/10.1016/j.biomaterials.2004.09.020.
125. Ma, C., et al. (2018). In vitro cytocompatibility evaluation of poly(octamethylene citrate) monomers toward their use in orthopedic regenerative engineering. *Bioactive Materials, 3*(1), 19–27. https://doi.org/10.1016/j.bioactmat.2018.01.002.
126. Torun Köse, G., Ber, S., Korkusuz, F. et al., (2003). Poly(3-hydroxybutyric acid-co-3-hydroxyvaleric acid) based tissue engineering matrices. *Journal of Materials Science: Materials in Medicine, 14*(2), 121–126. https://doi.org/10.1023/A:1022063628099.